JHEP

Published for SISSA by Springer

Received: April 26, 2020
Revised: September 11, 2020
Accepted: September 27, 2020
Published: November 10, 2020

"Lagrangian disks" in M-theory

Sebastián Franco,[a,b,c] **Sergei Gukov,**[d] **Sangmin Lee,**[e,f,g] **Rak-Kyeong Seong**[h] **and James Sparks**[i]

[a] *Physics Department,*
The City College of the CUNY, 160 Convent Avenue, New York, NY 10031, U.S.A.
[b] *Physics Program and* [c] *Initiative for the Theoretical Sciences,*
The Graduate School and University Center, The City University of New York,
365 Fifth Avenue, New York NY 10016, U.S.A.
[d] *Walter Burke Institute for Theoretical Physics, California Institute of Technology,*
Pasadena, CA 91125, U.S.A.
[e] *Center for Theoretical Physics, Seoul National University,*
Seoul 08826, Korea
[f] *Department of Physics and Astronomy, Seoul National University,*
Seoul 08826, Korea
[g] *College of Liberal Studies, Seoul National University,*
Seoul 08826, Korea
[h] *Yau Mathematical Sciences Center, Tsinghua University,*
100084 Beijing, China
[i] *Mathematical Institute, University of Oxford,*
Woodstock Road, Oxford, OX2 6GG, U.K.

E-mail: sfranco@ccny.cuny.edu, gukov@theory.caltech.edu, sangmin@snu.ac.kr, rakkyeongseong@gmail.com, sparks@maths.ox.ac.uk

Abstract: While the study of bordered (pseudo-)holomorphic curves with boundary on Lagrangian submanifolds has a long history, a similar problem that involves (special) Lagrangian submanifolds with boundary on complex surfaces appears to be largely overlooked in both physics and math literature. We relate this problem to geometry of coassociative submanifolds in G_2 holonomy spaces and to Spin(7) metrics on 8-manifolds with T^2 fibrations. As an application to physics, we propose a large class of brane models in type IIA string theory that generalize brane brick models on the one hand and 2d theories $T[M_4]$ on the other.

Keywords: Brane Dynamics in Gauge Theories, D-branes, M-Theory, Supersymmetric Gauge Theory

ArXiv ePrint: 1910.01645

https://doi.org/10.1007/JHEP11(2020)033

JHEP11(2020)033

Contents

1 Introduction and summary **1**

2 A simple instructive example **5**

3 Euler number anomaly **6**
- 3.1 Example 7
- 3.2 Type IIA interpretation and M-theory lift 7
- 3.3 QFT interpretation 10

4 New coassociative submanifolds **13**
- 4.1 Solving the Abel equation 16
- 4.2 Reversing the degree 24

5 Phase transitions and Spin(7) manifolds **25**

A Supersymmetry conditions for D6-branes **34**

B Calibration condition **34**

JHEP11(2020)033

1 Introduction and summary

A familiar setup, both in physics and in math, involves a (special) Lagrangian submanifold L in a Calabi-Yau 3-fold X together with bordered pseudoholomorphic curve Σ with boundary in L. Exploring all possible choices of Σ with fixed X and L is the main goal of "open Gromov-Witten theory" and plays an important role in counting disk instantons [1] which, in turn, are paramount for stability of string vacua.

In this paper we consider a much less explored version of this setup, which involves a similar triple, illustrated in figure 1:

$$\begin{array}{l} X: \text{Calabi-Yau 3-fold} \\ S: \text{complex surface} \\ L: \text{special Lagrangian} \end{array} \quad \rightsquigarrow \quad \begin{array}{l} X_7: G_2 \text{ holonomy} \\ M_4: \text{coassociative} \end{array} \quad \rightsquigarrow \quad X_8: \text{Spin(7) holonomy} \tag{1.1}$$

Here, X, S, and L are in a similar mutual relation as ingredients of open Gromov-Witten theory; namely, $S, L \subset X$ and L has boundary in S. As far as we know, moduli spaces of such special Lagrangians with boundary on S have not been studied in the previous literature.[1] Moreover, as we explain further below, the triple (X, S, L) defines a certain brane configuration in type IIA string theory that, upon lift to M-theory, yields a pair

[1] Surprisingly, even the linearized version of the problem [2] does not seem to have been pursued.

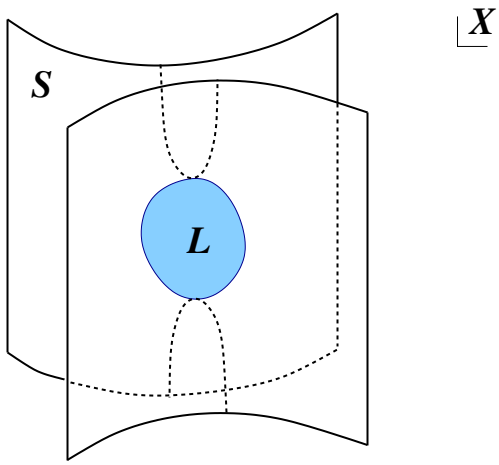

Figure 1. Our geometric setup involves a holomorphic surface S in a Calabi-Yau 3-fold X, and a special Lagrangian submanifold $L \subset X$ with boundary $\Sigma := \partial L \subset S$.

(X_7, M_4) of a G_2 holonomy manifold X_7 and a coassociative submanifold M_4 in it. A repeated application of this "M-theory lift" — denoted by squiggly arrows in (1.1) — similarly associates a Spin(7) holonomy manifold X_8 to the pair (X_7, M_4). As a result, the same triple (X, S, L) can be analyzed from several different perspectives, which correspond to different stages of (1.1).

In our models, we allow X and S to be compact or non-compact, whereas L is always assumed to be compact with non-trivial boundary

$$\Sigma := \partial L \ \subset \ S \tag{1.2}$$

In general, we allow L to have several connected components L_i, $i = 1, \ldots, \ell$, possibly taken with multiplicity $N_i \in \mathbb{Z}_+$.

Examples of (X, S, L) include the following natural choices:

- One can take $X = \mathbb{C}^* \times \mathbb{C}^* \times \mathbb{C}^* = T^*(T^3)$ and $L = T^3$ split into several "disks" $L_i \cong D^3$ (each of which has topology of a 3-ball) by a holomorphic surface $S \subset X$. These are the so-called brane brick models (BBMs) [3–5].

- More generally, one can take $X = T^*L$ to be the total space of the cotangent bundle over a 3-dimensional base manifold L, with a simple choice of L such as $\mathbb{R}^3$, T^3, S^3, $S^2 \times S^1$, etc. Each of the resulting spaces T^*L admits a complete Calabi-Yau metric.

- The previous class of examples contains the simplest Calabi-Yau 3-fold $X = \mathbb{C}^3$. Even with this choice of X, one can generate many interesting models by taking different hypersurfaces S defined by the zero locus of a polynomial $P(z_1, z_2, z_3)$:

$$S: \qquad P(z_1, z_2, z_3) = 0\,, \qquad (z_1, z_2, z_3) \in \mathbb{C}^3 \tag{1.3}$$

- Note, same Σ, defined (1.2) as a boundary of L, can bound several Lagrangians which, moreover, can be special Lagrangian. For a given $S \subset X$ and a fixed homology class

JHEP11(2020)033

$[\Sigma] \subset H_2(S)$, we denote the moduli space of such special Lagrangians by $\mathcal{M}(L; [\Sigma], S)$. Note, this moduli space may have several connected components. In the physical setup (1.7) defined by the triple (X, S, L) that we consider throughout this paper from various perspectives, this geometric moduli space can be identified with the physical moduli space of vacua / target space of the effective 2d $\mathcal{N} = (0, 2)$ theory on the $\mathbb{R}^2$ part of the D4-NS5 brane system[2]

$$\mathcal{M}\left(L;\ \overset{\text{fixed}}{[\Sigma]}, S\right) \ \cong\ \mathcal{M}_{\text{vacua}} \tag{1.4}$$

For example, let X be the "deformed conifold" defined by a quadratic equation

$$X: \qquad z_1^2 + z_2^2 + z_3^2 + z_4^2 = \epsilon\,, \qquad (z_1, z_2, z_3, z_4) \in \mathbb{C}^4 \tag{1.5}$$

A hypersurface defined by imposing an additional equation $z_4 = 0$ has topology $S \cong T^*S^2$ with a single non-trivial 2-cycle $\Sigma \cong S^2$ that bounds two special Lagrangian disks $L_1 \cong L_2 \cong D^3$ in X.

- Let $I_i \subset \mathbb{R}^3$ and $C_j \subset \mathbb{R}^3$ be a collection of intervals I_i and 2-planes C_j, such that all intervals are parallel to each other, with end-points on 2-planes, and such that C_j's are also mutually parallel and orthogonal to I_i's. Choosing a linear embedding $\mathbb{R}^3 \subset \mathbb{C}^2$ and taking a direct product of all elements in this arrangement $(\mathbb{C}^2, \{C_j\}, \{I_i\})$ with a 2-torus defines $X = \mathbb{C}^2 \times T^2$, $S = \sqcup_j (C_j \times T^2)$, and $L = \sqcup_i (I_i \times T^2)$ which corresponds to 2d compactification of the models studied in [6].

- Let X be the famous quintic Calabi-Yau 3-fold:

$$X: \qquad f(z_i) = 0\,, \qquad (z_1, \ldots, z_5) \in \mathbb{C}\mathbf{P}^4 \tag{1.6}$$

where $f(z_i)$ is a homogeneous polynomial of degree 5. Imposing an extra linear relation[3] cuts out a degree-5 surface of general type, which is simply-connected and has $b_2^+(S) = 9$, $b_2^-(S) = 44$. Since $b_2(X) = 1$, there are many primitive[4] homology classes in the 53-dimensional lattice $H_2(S; \mathbb{Z})$ that are trivial in X, thus providing many potential candidates for Σ that bound Lagrangian "disks" $L \subset X$.

While the input data for each of our models is the triple (X, S, L), the output can be summarized either as a pair (X_7, M_4) of a G_2 holonomy 7-manifold X_7 with a coassociative

[2] Relegating a more detailed discussion of various aspects of the D4-NS5 brane system (1.7) to later parts of the paper, here we note that compactification of type IIA string theory on a generic Calabi-Yau 3-fold X (with irreducible holonomy group) preserves 8 out of 32 real supercharges. Then, introducing NS5-branes into (1.7) breaks half of the remaining supercharges. Finally, adding D4-branes preserves a half of the remaining 4 supercharges, which are both chiral with respect to two-dimensional space $\mathbb{R}^2$ and whose (anti)commutator generates a Poincaré symmetry along the $\mathbb{R}^2$. The resulting supersymmetry algebra is 2d $\mathcal{N} = (0, 2)$ chiral supersymmetry algebra (where the two supercharges are conventionally taken to be right-moving).

[3] which, without loss of generality, we can assume to be $z_5 = 0$.

[4] A class in $H^2(S; \mathbb{Z}) \cong H_2(S; \mathbb{Z})$ is called primitive if its wedge product (or, equivalently, a contraction) with the Kähler form vanishes. This condition is necessary for Σ to be a Lagrangian 2-manifold in S.

JHEP11(2020)033

submanifold M_4, or as an 8-manifold X_8 of Spin(7) holonomy. They are produced from the input data via the map $\rightsquigarrow$ that we call "M-theory lift," because (X_7, M_4) is the result of lifting to eleven dimensions the following type IIA brane configuration[5]

$$\begin{array}{rccc} \text{space-time:} & \mathbb{R}^4 & \times & X \\ & \cup & & \cup \\ \text{NS5-branes:} & \mathbb{R}^2 & \times & S \\ \text{D4-branes:} & \mathbb{R}^2 & \times & L \end{array} \tag{1.7}$$

whereas X_8 is similarly produced [9, 10] from D6-branes supported on $\mathbb{R}^3 \times M_4$ in type IIA space-time $\mathbb{R}^3 \times X_7$. This M-theory lift of D6-branes supported on $\mathbb{R}^3 \times M_4$ is an auxiliary problem from the viewpoint of our main setup (1.7) and is modeled after [7, 8], where analogous M-theory lift of D6-branes on special Lagrangian 3-manifolds was considered. Note, when part of the brane world-volume is embedded in a special holonomy manifold as a calibrated submanifold, the corresponding (part of) the world-volume theory is automatically topologically twisted [11–13].

When the Calabi-Yau 3-fold X is compact and has irreducible SU(3) holonomy group, a compactification of type IIA string theory on X produces a 4d $\mathcal{N} = 2$ effective supergravity theory coupled to matter. In this theory, a configuration of NS5 and D4-branes as in (1.7) engineers a $\frac{1}{4}$-BPS surface operator, which preserves $\mathcal{N} = (0, 2)$ supersymmetry on its two-dimensional world-volume $\mathbb{R}^2$. Since the M-theory lift of this configuration has to preserve the same symmetry and supersymmetry, we quickly learn that it is given by M5-branes wrapped on a coassociative cycle in a G_2 holonomy manifold,

$$\begin{array}{rccc} \text{space-time:} & \mathbb{R}^4 & \times & X_7 \\ & \cup & & \cup \\ \text{M5-branes:} & \mathbb{R}^2 & \times & M_4 \end{array} \tag{1.8}$$

When a certain anomaly discussed in section 3 vanishes, the topology of the G_2 manifold is simply $X_7 \cong S^1 \times X$, and[6]

$$M_4 = (S \setminus \Sigma) \cup_{\Sigma \times S^1} \left(L \times S^1\right) \tag{1.9}$$

When the anomaly of section 3 is non-trivial, the story involves additional ingredients and the geometry of X_7 and M_4 becomes more interesting. In particular, X_7 is topologically

[5] It would be interesting to understand under what conditions the G_2 holonomy manifold X_7 exists globally. We expect that, in "local models" (i.e. when X is non-compact) it exists whenever this type IIA brane configuration is free of anomalies, such as those discussed in section 3. This is supported by examples considered in this paper and in earlier works [7, 8] where similar brane configurations were lifted to G_2 holonomy metrics in M-theory. On the other hand, brane models with compact X involve dynamical gravity and moduli fields which often exhibit a runaway behavior and/or drive the system into a strongly coupled regime, where the entirely classical description based on geometry may not be possible. In such situations we hope that exploring brane disk models (1.7) further can shed light on the set of conditions under which X_7 has large volume and bounded curvature, so that a description in terms of classical geometry is valid globally on X_7.

[6] Note, when $L = S^3 \setminus K$ this operation is nothing but the standard knot surgery in S [14]. See e.g. [15] for physics-friendly introduction to various elements of 4-manifold topology that will be useful to us here.

JHEP11(2020)033

no longer a product $S^1 \times X$, but rather a non-trivial circle fibration:

$$\begin{array}{ccc} S^1 & \longrightarrow & X_7 \\ & & \downarrow \\ & & X \end{array} \tag{1.10}$$

Similarly, X_8 is a circle fibration over X_7 or, equivalently, a torus fibration over X:

$$\begin{array}{ccc} T^2 & \longrightarrow & X_8 \\ & & \downarrow \\ & & X \end{array} \tag{1.11}$$

Indeed, starting with a G_2 holonomy space X_7 and a coassociative submanifold $M_4 \subset X_7$, one can consider an (auxiliary) physical system — similar to (1.7) but not directly related to it — which involves type IIA string theory with ten-dimensional space-time $\mathbb{R}^3 \times X_7$ and D6-branes supported on $\mathbb{R}^3 \times M_4$. Because D6-branes lift to components of the eleven-dimensional metric in M-theory, this D6-brane configuration lifts to a purely geometric background in M-theory. Moreover, it preserves 3d Poincaré symmetry and only two real supercharges, which means that the 11d background must be of the form $\mathbb{R}^3 \times X_8$, where X_8 has Spin(7) holonomy. This allows to relate and reformulate the original moduli problem for Lagrangian "disks" L with boundary on $S \subset X$ as a potentially more tractable and better understood problem of moduli of Spin(7) metrics or moduli of coassociative submanifolds in G_2 holonomy spaces. We hope that families of new Spin(7) metrics on (1.11) labeled by (X, S, L) can be constructed using methods similar to those in [16, 17], where many new G_2 analogues of Taub-NUT spaces were found.

The paper is organized as follows. We start in section 2 with a simple example of the D4-NS5 brane model (1.7). In section 3 we describe a new chiral anomaly on 4d boundary of D4-branes. In section 4 we construct new coassociative submanifolds in $\mathbb{R}^3 \times$ Taub-NUT which are ALF generalizations of the ALE coassociatives in $\mathbb{R}^7$ constructed by Harvey and Lawson [18]. In section 5 we analyze in detail the physics of one of the D4-NS5 brane models (1.7) and make a proposal for the 2d $\mathcal{N} = (0, 2)$ effective theory. In particular, via lift to M-theory on a G_2 manifold, it gives us a concrete description of the moduli space (1.4) in that brane model:

$$\mathcal{M}\,(L; [\Sigma], S) \;\cong\; \mathcal{M}_{\text{vacua}} = \{(z, w) \in \mathbb{C}^2 \mid zw = 0\} \tag{1.12}$$

2 A simple instructive example

If one wants to construct the simplest model labeled by (X, S, L), for the choice of X nothing can be simpler than $\mathbb{C}^3$. For the choice of complex surface S, it is natural to take the zero locus (1.3) of a polynomial $P(z_1, z_2, z_3)$. Since we want S to contain at least one non-trivial 2-cycle Σ, the degree of $P(z_1, z_2, z_3)$ has to be at least 2. So, in our simple toy model we make a symmetric choice

$$S: \qquad P(z_1, z_2, z_3) = z_1^2 + z_2^2 + z_3^2 - \epsilon^2 = 0\,, \qquad (z_1, z_2, z_3) \in \mathbb{C}^3 \tag{2.1}$$

JHEP11(2020)033

which has the added benefit of an extra symmetry $\mathrm{SU}(2) \cong \mathrm{SO}(3)$. Without loss of generality, we can take the constant ϵ to be real and positive. Topologically, S is a line bundle $\mathcal{L} = \mathcal{O}(-2)$ over $\mathbb{C}\mathbf{P}^1$. In particular, S admits a non-contractible 2-cycle $\Sigma \cong S^2$ which, of course, is contractible in the ambient space $X = \mathbb{C}^3$. The 2-cycle Σ can be described explicitly by the same equation (2.1) with (z_1, z_2, z_3) restricted to the real slice:

$$\Sigma \cong S^2 \ : \qquad \vec{x}^2 = \epsilon^2 \,, \quad \vec{y} = 0 \,, \quad \vec{x}, \vec{y} \in \mathbb{R}^3 \quad (z_k = x_k + i y_k) \tag{2.2}$$

In the ambient space $X = \mathbb{C}^3$ it can be "filled in" by a disk — or, rather, by a 3-dimensional ball — with boundary Σ:

$$L \ : \qquad \vec{x}^2 \leq \epsilon^2 \,, \quad \vec{y} = 0 \tag{2.3}$$

It is easy to check that L is, in fact, special Lagrangian with respect to the flat Calabi-Yau structure on $X = \mathbb{C}^3$:

$$\Omega = dz_1 \wedge dz_2 \wedge dz_3 \,, \qquad J = \frac{i}{2} dz_1 \wedge d\bar{z}_1 + \frac{i}{2} dz_2 \wedge d\bar{z}_2 + \frac{i}{2} dz_3 \wedge d\bar{z}_3 \tag{2.4}$$

Once we introduced the key players, X, S, and L, they appear to define a perfectly sensible configuration of NS5 and D4-branes (1.7) with world-volumes $\mathbb{R}^2 \times S$ and $\mathbb{R}^2 \times L$, respectively. This choice of (X, S, L), however, suffers from an important anomaly. As we explain in the next section, this anomaly can be easily cured. However, as it stands, the triple (X, S, L) introduced here does not define a consistent model and, in particular, does not admit a lift (1.1) to a coassociative submanifold $M_4 \subset X_7$ or to a Spin(7) manifold X_8.

3 Euler number anomaly

The simple choice of (X, S, L) introduced in the previous section is a good example to illustrate an important anomaly in our class of models, which in general takes values in

$$H^2(\Sigma, \mathbb{Z}) \ \cong \ H_0(\Sigma, \mathbb{Z}) \tag{3.1}$$

Specifically, for each connected component of Σ, there is a potential $\mathbb{Z}$-valued anomaly given by the self-intersection of that component in the complex surface S:

$$n_i = \Sigma_i \cdot \Sigma_i \,, \qquad i = 1, \ldots, \dim H_0(\Sigma, \mathbb{Z}) \tag{3.2}$$

This anomaly can be seen both physically and geometrically. In this section we begin by illustrating the anomaly for the simple example in section 2, focusing on the M-theory geometric perspective. In section 3.2 we then present a general discussion of the anomaly in type IIA string theory, how this lifts to the M-theory picture, and how the anomaly can be cured (in a more or less canonical way). Finally, section 3.3 presents the QFT manifestation of the anomaly in our class of models.

JHEP11(2020)033

3.1 Example

In our simple example (2.1)–(2.3), the lift to M-theory involves a 7-manifold of G_2 holonomy, X_7, which topologically is simply a product of X and the M-theory circle S^1. This is a general feature of any type IIA background that does not involve D6-branes or RR 2-form fluxes. Likewise, a lift of the Lagrangian disk (2.3) is also a product $L \times S^1$, which is automatically coassociative in $X_7 = X \times S^1$ with respect to the natural G_2 structure (4.1). The 4-manifold $L \times S^1$, however, has boundary $\Sigma \times S^1$ and needs something to end on. Indeed, both NS5 and D4-branes turn into M5-branes upon M-theory lift. And, just like in type IIA theory the NS5-brane (2.1) serves as a boundary condition for the D4-brane (2.3), in M-theory they join into one single 4-manifold since the M-theory lift of the NS5-brane is simply $S \subset X_7$.

Now we are starting to see the anomaly or, at least, its geometric manifestation. The boundary of $L \times S^1$ is $\Sigma \times S^1$. The boundary of $S \setminus \Sigma$ locally looks very similar; the normal sphere bundle to $\Sigma \subset S$ is just a circle S^1 bundle. However, when the normal bundle is non-trivial, the boundary of $S \setminus \Sigma$ is a non-trivial S^1 bundle over Σ of degree n given by the self-intersection (3.2). Therefore, when $n \neq 0$, we cannot simply glue $S \setminus \Sigma$ and $L \times S^1 \subset X_7$ into a single 4-manifold (1.9) along their boundaries since these boundaries are different. This is precisely the case in our simple example, where $n = \Sigma \cdot \Sigma = -2$.

3.2 Type IIA interpretation and M-theory lift

The geometric anomaly just illustrated may be seen from the type IIA brane perspective as follows. On the worldvolume of the NS5-brane propagates a periodic scalar field φ, where we normalize φ to have period 2π. This worldvolume theory arises from dimensional reduction of the M5-brane theory [19], where the NS5-brane is transverse to the M-theory circle direction, S^1_M. The scalar φ then corresponds to motion of the M5-brane in that direction. On the other hand, a D4-brane ending on an NS5-brane acts as a magnetic source for this scalar [6]. In our set-up, recall from (1.7) that the NS5-brane worldvolume is $\mathbb{R}^2 \times S \subset \mathbb{R}^4 \times X$, where the D4-brane wrapped on $\mathbb{R}^2 \times L$ shares the $\mathbb{R}^2$ directions with the NS5-brane. Suppressing the common $\mathbb{R}^2$ directions, the end of the D4-brane is then $\partial L = \Sigma \subset S$. Since this has codimension 2 in S, it is linked by a circle S^1. As one goes around such a transverse $S^1 \subset S$, the periodic scalar φ winds once around 2π, so that $\mathbb{R}^2 \times \Sigma$ is effectively the locus of a "vortex" for the φ field.

We may describe this in more detail as follows. The scalar φ enters the worldvolume theory of the NS5-brane via its gauge-invariant curvature [19]

$$\mathcal{F}_1 \equiv d\varphi - \iota^* C_1 \tag{3.3}$$

where C_1 denotes the RR 1-form potential, and $\iota : \mathbb{R}^2 \times S \hookrightarrow \mathbb{R}^4 \times X$ denotes the embedding of the NS5-brane into space-time, with ι^* a pull-back to the worldvolume. Of course, we might *a priori* choose to turn off this RR potential, setting $C_1 = 0$, since neither the NS5-brane nor D4-brane source it. However, we shall see shortly that in general there is an anomaly that forces us to turn it on.

JHEP11(2020)033

To say that $\Sigma \subset S$ is a magnetic source for φ means that φ winds once around 2π as it moves around an S^1 linking Σ. That is,

$$\int_{S^1} d\varphi = 2\pi \tag{3.4}$$

where $S^1 \subset \mathbb{R}^2$ is a positive constant radius circle in the $\mathbb{R}^2$ normal directions to Σ in S. More generally for k D4-branes the winding is $2\pi k$. Notice equivalently we may write

$$d^2\varphi = 2\pi\delta_2 \tag{3.5}$$

where δ_2 is a delta-function representative of the Poincaré dual of $\Sigma \subset S$, i.e. δ_2 is a closed 2-form on S which restricts to a Dirac delta-function times the volume form in the normal $\mathbb{R}^2$ directions of Σ.

Although in general neither φ nor the RR potential $\iota^* C_1$ are globally defined on the NS5-brane worldvolume, the 1-form $\mathcal{F}_1$ defined in (3.3) is a gauge-invariant curvature form. Taking the exterior derivative of this latter equation, in the presence of a D4-brane ending on the NS5-brane, gives

$$d\mathcal{F}_1 = 2\pi\delta_2 - \iota^* G_2 \tag{3.6}$$

where $G_2 = dC_1$ is the RR 2-form flux. Since the left hand side is exact, its cohomology class in $H^2(S, \mathbb{R})$ is zero, and we deduce the equality of cohomology classes

$$[\iota^* G_2] = 2\pi[\delta_2] \in H^2(S, \mathbb{R}) \tag{3.7}$$

In other words, when the end of the D4-brane $\Sigma \subset S$ has a Poincaré dual δ_2 that defines a non-trivial cohomology class in $H^2(S, \mathbb{R})$, one must *necessarily* turn on a RR G_2 field obeying (3.7): to not do so leads to our anomaly.

Let us examine this further. We denote the normal bundle of Σ inside S as $N\Sigma$, which is a complex line bundle. Such line bundles are classified by their first Chern class, which here lies in $H^2(\Sigma, \mathbb{Z}) \cong \mathbb{Z}^{b_0(\Sigma)}$, where as in (3.1) $b_0(\Sigma) = \dim H_0(\Sigma, \mathbb{Z})$ is the number of connected components of Σ. For the ith component Σ_i we may then identify $N\Sigma_i = \mathcal{O}(n_i)$ as the line bundle over Σ_i of Euler number $n_i \in \mathbb{Z}$. More abstractly, for each $i = 1, \ldots, b_0(\Sigma)$ the Poincaré dual δ_2 represents the generator of the compactly supported cohomology $[\delta_2]_{\rm cpt} = 1 \in H^2_{\rm cpt}(N\Sigma_i, \mathbb{Z}) \cong H^0(\Sigma_i) \cong \mathbb{Z}$. This generator is also known as the *Thom class*. There is a natural mapping from $\mathbb{Z} \cong H^2_{\rm cpt}(N\Sigma_i, \mathbb{Z}) \to H^2(N\Sigma_i, \mathbb{Z}) \cong H^2(\Sigma_i, \mathbb{Z}) \cong \mathbb{Z}$ where the map simply forgets the compact support condition. This maps the Thom class $1 \in \mathbb{Z}$ to the Euler number $n_i \in \mathbb{Z}$. Putting all this together, we may integrate (3.6) over Σ_i to obtain

$$\int_{\Sigma_i} \frac{G_2}{2\pi} = n_i \tag{3.8}$$

Recall that geometrically G_2 is the curvature of the M-theory circle bundle over space-time. Thus (3.8) says that we must fiber the M-theory circle bundle in such a way that the Euler number of this fibration over Σ_i, which is the left hand side of (3.8), is the same as the self-intersection number $n_i = \Sigma_i \cdot \Sigma_i$, which is also the Euler number of the normal bundle $N\Sigma_i$ of Σ_i in S. There are two ways to generate such a flux in our set-up, where

JHEP11(2020)033

recall that space-time is $\mathbb{R}^4 \times X$, with X a Calabi-Yau 3-fold: we may turn on RR 2-form flux on X, and/or introduce D6-branes into the space-time, which magnetically source such a flux. In order to preserve supersymmetry, the RR 2-form flux on X should be Hodge type $(1,1)$, and D6-branes should wrap a special Lagrangian $L_{D6} \subset X$ and are space-filling in the $\mathbb{R}^4$ directions. The lift of X to M-theory is then not simply a product $X \times S^1_M$, but rather the total space X_7 a non-trivial circle fibration over X, (1.10), which degenerates at D6-brane loci. Supersymmetry implies that X_7 is a G_2 holonomy manifold. Notice that in the simple case that $X = \mathbb{C}^3$, as in the example in section 2, since $H^2(X, \mathbb{Z}) = 0$ we must necessarily introduce D6-branes to source the required flux on the left hand side of (3.8). We shall return to discuss this example at the end of the next subsection.

The condition (3.8) has a very elegant geometric interpretation, once we lift the NS5-brane and D4-brane configuration to M-theory. Both objects descend from an M5-brane, where the NS5-brane is transverse to the M-theory circle while the D4-brane wraps the circle. Since the D4-brane ends on the NS5-brane, the configuration should lift to a *single* M5-brane wrapped on a 4-manifold M_4 in M-theory. The classical picture of the D4-brane ending on a definite submanifold $\Sigma \subset S$ inside the NS5-brane is not quite accurate, due to the resulting distortion near to this locus. Let us examine the lift of both branes away from the intersection locus Σ. The NS5-brane wraps $S \setminus \Sigma$, which near to a connected component Σ_i looks like $N\Sigma_i \setminus \Sigma_i \cong I \times M_3$, where $I = (0, \epsilon]$ is an interval and M_3 is the total space of a degree n_i circle bundle over Σ_i

$$M_3 \quad = \quad \begin{array}{c} S^1 \\ \downarrow \text{ deg. } n_i \\ \Sigma_i \end{array} \tag{3.9}$$

On the other hand, the D4-brane wraps $L \setminus \Sigma$, which near to the ith end looks like $I \times \Sigma_i$. On lifting to M-theory, the M-theory circle fibres over this latter geometry to give the M5-brane worldvolume, and (3.8) says that the total space of this S^1_M bundle over $I \times \Sigma_i$ is also precisely $I \times M_3$. The condition (3.8) thus ensures that the boundaries of these two neck regions, around where the NS5-brane and D4-brane meet, lift to the same 3-manifold M_3 in M-theory, and as in [6] these are glued together to produce a single smooth M5-brane by connecting the necks via a small "tube" $[-\epsilon, \epsilon] \times M_3$. The M5-brane is then wrapped on the smooth 4-manifold

$$M_4 = (S \setminus \Sigma) \cup_{M_3} (S^1_M \to L \setminus \Sigma) \tag{3.10}$$

On the other hand, without the addition of the RR 2-form flux the boundaries are different 3-manifolds, so we cannot simply glue them together. We saw this for our explicit example in section 3.1.

We conclude this subsection with a few more general remarks. Suppose one has a submanifold S in space-time over which there is a non-trivial RR 2-form flux, i.e. the pull-back $[\iota^* G_2] \neq 0 \in H^2(S, \mathbb{R})$. Then one *cannot* wrap an NS5-brane over S. Geometrically, this is because the NS5-brane is an M5-brane transverse to the M-theory circle, and thus the M-theory circle bundle over S must have a global section. But this is true if and only

JHEP11(2020)033

if the S^1_M bundle is trivial over S, and hence $[\iota^* G_2] = 0 \in H^2(S, \mathbb{R})$. One can see these same facts also from the point of view of the NS5-brane worldvolume theory, specifically from the curvature form $\mathcal{F}_1 = d\varphi - \iota^* C_1$. Since the worldvolume periodic scalar φ is also a section of the same M-theory circle bundle over S, this scalar field exists as a global function on S if and only if that bundle is trivial. In that case the Bianchi identity for $\mathcal{F}_1$ reads $d\mathcal{F}_1 = -\iota^* G_2$, again impling that $[\iota^* G_2] = 0 \in H^2(S, \mathbb{R})$.

If instead $[\iota^* G_2] \neq 0 \in H^2(S, \mathbb{R})$, the best one can do is to remove a submanifold $\Sigma \subset S$ that is Poincaré dual to $[\iota^* G_2/2\pi]$. By construction, the M-theory circle bundle is then trivial over $S \setminus \Sigma$, and an NS5-brane can wrap this locus. Of course, physically we may then require a D4-brane to end on the locus Σ, thus satisfying (3.6), and this system then lifts to a single smooth M5-brane, without additional boundaries. In this case the worldvolume scalar φ is not defined at the locus $\Sigma \subset S$ due to the winding by 2π in (3.4), just as the angular coordinate θ is not defined at the origin of $\mathbb{R}^2$ in plane polar coordinates.

Similar remarks apply to a D2-brane with a fundamental string ending on it, which lifts to an M2-brane. In particular, the D2-brane worldvolume theory contains a periodic scalar corresponding to motion of the M2-brane in the M-theory circle direction. In three dimensions a periodic scalar is dual to an Abelian gauge field, which in this case is nothing but the usual U(1) gauge field on a D-brane. A fundamental string ending on a D-brane is of course an electric source for this gauge field, or equivalently for the D2-brane a magnetic source for the dual periodic scalar.

3.3 QFT interpretation

Now let us discuss the QFT origin and interpretation of this "Euler number anomaly." Just like in its geometric manifestation, the crucial ingredient is the neck region along which $S \setminus \Sigma$ and $L \times S^1$ are supposed to be joined. Recall from the previous subsection that near the ith connected component of this neck region, $S \setminus \Sigma$ looks like $I \times M_3$, where $I = (0, \epsilon]$ and M_3 is the total space of a degree n_i circle bundle over Σ_i in (3.9). Let us look more closely at the physics of a five-brane near this neck region, i.e. a five-brane on $\mathbb{R}^2 \times I \times M_3$. More generally, we can consider N five-branes supported on $\mathbb{R}^2 \times I \times M_3$.

Since $I \times M_3$ is part of the curved 4-manifold along which the five-brane is topologically twisted, a priori the interval I is not quite on the same footing as the $\mathbb{R}^2$ part of the five-brane world-volume. However, since I admits a flat metric, and since in flat space the full physical and topological theories are the same, we can treat $\mathbb{R}^2 \times I$ as a space-time of the 3d physical theory obtained by compactifying a five-brane on M_3.

This physical 3d theory has $\mathcal{N} = 2$ supersymmetry and is usually denoted $T[M_3]$. It is defined for any 3-manifold M_3, but in our applications here we only need to know this theory for very special 3-manifolds of the form (3.9). For example, when $\Sigma = S^2$, as in (2.2), we have $M_3 = L(n, 1)$ and $T[M_3, G]$ is the following "Lens space theory" [15, 20]:

$$T[L(n,1), G] \quad = \quad \begin{array}{c} \text{3d } \mathcal{N} = 2 \text{ super-Chern-Simons} \\ \text{with } G_n \text{ and an adjoint chiral} \end{array} \tag{3.11}$$

The important aspect of this theory is that it involves a Chern-Simons coupling for the gauge group G at level n.

JHEP11(2020)033

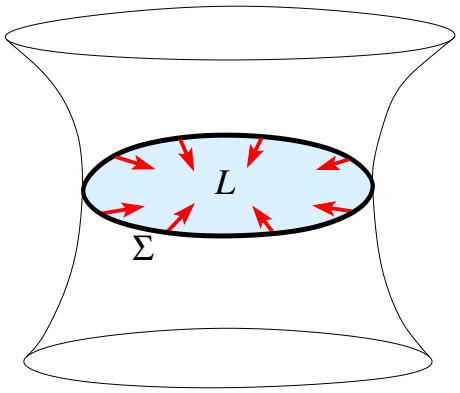

Figure 2. An illustration of the anomaly inflow from the boundary into the bulk of the D4-brane world-volume theory.

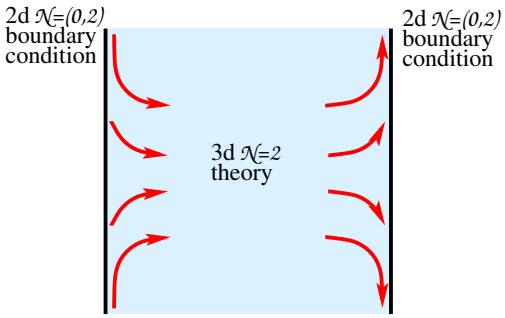

Figure 3. An illustration of the anomaly inflow in 3d $\mathcal{N} = 2$ theory with 2d $\mathcal{N} = (0, 2)$ boundary conditions. For example, if one boundary carries charged chiral fermions whose anomaly is compensated by Chern-Simons couplings of the 3d bulk theory, a similar mechanism must be at work at the other boundary.

In our simple example (2.3), the interval $I = (0, \epsilon]$ is parametrized by the radial coordinate $r = |\vec{x}|$, and the 3d theory we described is a result of the reduction of the five-brane world-volume theory on the M-theory circle and $\Sigma = S^2$ (or, more precisely, on an S^1 bundle over Σ). At the end-points of the interval I we need to impose 2d boundary conditions, which must preserve $\mathcal{N} = (0, 2)$ supersymmetry because this is the amount of supersymmetry preserved by the brane configuration.

The 2d $\mathcal{N} = (0, 2)$ boundary conditions in question have a geometric origin: at one end of the interval the boundary condition is determined by the 4-manifold $S \setminus \Sigma$. This is where D4-brane runs into NS5-brane. At the other end of the interval, the boundary condition is determined by what happens at the limit $r = 0$. The resulting system looks like a 3d $\mathcal{N} = 2$ theory (3.11) sandwiched by 2d $\mathcal{N} = (0, 2)$ boundary conditions, precisely of the type studied in [15] and illustrated in figure 3.

In particular, when $n \neq 0$, there is a non-trivial anomaly inflow that also played an important role in [15]. And, what our above analysis shows is that the boundary condition where the D4-brane runs into the NS5-brane infuses n units of anomaly compensated by the Chern-Simons coupling of the 3d theory and also carried to the other boundary. Therefore, the other boundary condition (at $r = 0$ in our simple example) should also carry n units

JHEP11(2020)033

of anomaly, i.e. it should carry chiral degrees of freedom charged under G (= gauge group of D4-brane theory).

The original system of NS5 and D4-branes has no such degrees of freedom at $r = 0$. Therefore, it is anomalous. However, our analysis in the previous subsection also suggests what one should do in order to cancel this anomaly. The simplest possibility is to add n D6-branes that, geometrically, would replace a product with the M-theory circle by a non-trivial bundle and, physically, would produce n charged chiral fermions at the 2-dimensional intersection of the D4 and D6-branes (the lowest modes of D4-D6 open strings). As mentioned earlier, in general another possibility is to turn on RR 2-form flux. In this paper, we mostly consider the first option.

The extra D6-branes that we need to add in order to cancel the Euler number anomaly (when $n \neq 0$) should have the following properties. First, their 7-dimensional world-volume should intersect the world-volume $\mathbb{R}^2 \times L$ of the D4-branes along $\mathbb{R}^2$ (times a point in L, which in our simple example is best to be chosen at $r = 0$ in order to preserve SU(2) symmetry of the background). Second, the D6-branes must preserve the unbroken supersymmetry of the original brane system (1.7). These two conditions imply that D6-branes must be supported on $\mathbb{R}^4 \times L_{D6}$, where $L_{D6} \subset X$ is a special Lagrangian submanifold calibrated by the 3-form $\mathrm{Im}(\Omega)$, provided L is calibrated by $\mathrm{Re}(\Omega)$:

$$\begin{array}{ll} \text{space-time:} & \mathbb{R}^4 \times X \\ \hline \text{NS5-branes:} & \mathbb{R}^2 \times S \\ \text{D4-branes:} & \mathbb{R}^2 \times L \\ \text{D6-branes:} & \mathbb{R}^4 \times L_{D6} \end{array} \tag{3.12}$$

See appendix A for details.

In our model example from section 2, a special Lagrangian $L_{D6} \subset \mathbb{C}^3$ that meets (2.3) at $\vec{x} = 0$ and is calibrated by $\mathrm{Im}(\Omega)$ is a three-dimensional plane:

$$L_{D6} \quad : \qquad \vec{y} \in \mathbb{R}^3\,, \quad \vec{x} = 0 \tag{3.13}$$

In its presence, the corresponding M-theory lift of (3.12) is of the form (1.10):

$$X_7 = \mathbb{R}^3 \times \mathrm{TN}_n \tag{3.14}$$

with a coassociative submanifold, cf. (1.9),

$$M_4 = (S \setminus \Sigma) \cup_{M_3} \mathrm{Cone}(M_3) \tag{3.15}$$

where M_3 is the 3-manifold introduced in (3.9). Since in our example the complex surface S is itself asymptotically a cone on M_3, and $n = -2$, it follows that $M_4 = \mathrm{Cone}(M_3) \cong \mathbb{R}^4/\mathbb{Z}_2$.

Note, instead of D4-branes supported on Lagrangian disks (2.3), illustrated in figure 2, one can consider non-compact D4-branes supported on the "disk complement,"

$$L \quad : \qquad \vec{x}^2 \geq \epsilon^2\,, \quad \vec{y} = 0 \tag{3.16}$$

Although this option may seem less natural for the purpose of building a dynamical 2d gauge theory on D4-brane world-volume, it does have very interesting physics, as will be

JHEP11(2020)033

discussed in section 5. Brane models with such non-compact D4-branes also exhibit the familiar Euler number anomaly which, much like (3.2), can be expressed in terms of the D4-brane boundary components $\Sigma_i \subset S$. However, since the orientation of the boundary of a D4-brane on a "disk complement" is reversed compared to that supported on a Lagrangian disk, the Euler number anomaly in these two cases differs by sign,

$$n_i = -\Sigma_i \cdot \Sigma_i \tag{3.17}$$

which is equivalent to $n_i \to -n_i$. In our simple class of models with n D6-branes, replacing compact D4-branes on Lagrangian disks by non-compact D4-branes supported on disk complements (3.16) leads to coassociative submanifold in (3.14) that are double-ended cones on

$$S^3/\mathbb{Z}_n \sqcup -S^3/\mathbb{Z}_n \tag{3.18}$$

When the apex is smoothed out, these become topologically

$$M_4 \cong \mathbb{R} \times S^3/\mathbb{Z}_n \tag{3.19}$$

The next section offers an explicit construction of such coassociative submanifolds.

4 New coassociative submanifolds

When $X_7 = S^1 \times X$, the associative and coassociative forms on X are

$$\begin{aligned} \Phi &= J \wedge d\psi - \mathrm{Im}(\Omega) \\ \Psi &= \frac{1}{2} J \wedge J + \mathrm{Re}(\Omega) \wedge d\psi \end{aligned} \tag{4.1}$$

where ψ is a coordinate on S^1. In particular, it is clear that, given a special Lagrangian $L \subset X$ calibrated by $\mathrm{Re}(\Omega)$ and a complex surface $S \subset X$, both $S^1 \times L$ and S are individually coassociative in X_7.

We are interested in a coassociative 4-manifold $M_4 \subset X$ defined by "smoothing" of $S^1 \times L$ and S near the "neck" region $S \cap (L \times S^1) = S^1 \times \Sigma$. As we saw in section 3, such smoothing is possible only if the self-intersection of Σ inside S vanishes. If that is the case, M_4 is given by the (deformation of) eq. (1.9). When the self-intersection of Σ in S is non-zero, we need to replace $X_7 = S^1 \times X$ by a non-trivial circle bundle (1.10), such that

$$X_7/S^1 \cong X \tag{4.2}$$

Motivated by our discussion in sections 2 and 3, let us analyze more carefully how this works in the class of examples with $X = \mathbb{C}^3$ and one component (3.13) of the codimension-4 fixed point set supported on $\mathbb{R}^3 \subset \mathbb{C}^3$. For a circle bundle of degree n, the total space (3.14)

$$X_7 = \Lambda^{2,+}(\mathrm{TN}_n) \cong \mathbb{R}^3 \times \mathrm{TN}_n \tag{4.3}$$

carries a G_2 structure determined by the first relation,

$$\Phi = dy_1 \wedge dy_2 \wedge dy_3 - \sum_{i=1}^{3} \omega_i \wedge dy_i \tag{4.4}$$

JHEP11(2020)033

where ω_i are self-dual 2-forms on the Taub-NUT space TN_n of "charge" n. The standard way to write a hyper-Kähler metric on the Taub-NUT space, which is ideally suited for our application to (3.14) with coordinates $(\vec{x}, \vec{y}, \psi)$, is

$$ds^2(\mathrm{TN}_n) = H d\vec{x} \cdot d\vec{x} + H^{-1} \left(d\widetilde{\psi} + \vec{\chi} \cdot d\vec{x} \right)^2 \tag{4.5}$$

where $H(\vec{x})$ is the harmonic function on $\mathbb{R}^3 \cong \mathrm{TN}_n/S^1$, such that

$$\nabla \times \vec{\chi} = \nabla H \,. \tag{4.6}$$

Equivalently, $d\chi = *_3 dH$, where $*_3$ is the Hodge dual with respect to the flat metric of $\mathbb{R}^3$ parametrized by $\vec{x}$. In these conventions, the triplet of the self-dual 2-forms on TN_n that appear in (4.4) can be explicitly written as

$$\vec{\omega} = \left(d\widetilde{\psi} + \vec{\chi} \cdot d\vec{x} \right) \wedge d\vec{x} - \frac{1}{2} H \, (d\vec{x} \times d\vec{x}) \,, \tag{4.7}$$

where $(d\vec{x} \times d\vec{x})^i = \epsilon^{ijk} dx^j \wedge dx^k$.

In order to preserve the SO(3) symmetry of the triple (X, S, L) in our main example (2.1)–(2.3), let us choose the harmonic function H in the form

$$H = B + \frac{n}{|\vec{x}|} = B + \frac{n}{r} \,, \tag{4.8}$$

where the constant B is related to the ratio between the radius of the M-theory circle and the eleven dimensional Planck scale. Then, the expression (4.4) is invariant under the SO(3) symmetry, which acts on ω_i and dy_i in the same way.

Note, all of our ingredients in the original setup (2.1)–(2.3) can be easily described in the coordinates $\vec{x}$ and $\vec{y}$. Namely, the complex surface (2.1) looks like

$$S \ : \qquad \vec{x}^2 - \vec{y}^2 = \epsilon^2 \,, \qquad \vec{x} \cdot \vec{y} = 0 \,, \tag{4.9}$$

and $\Sigma \cong S^2$ was already described in (2.2) as a sphere in $\vec{x}$-plane of radius ϵ. The Lagrangian L is a 3-ball ("disk") within this plane, whereas the Lagrangian $L_{D6} \cong \mathbb{R}^3$ is a copy of $\vec{y}$-plane at $\vec{x} = 0$, cf. (3.13).

In order to construct new coassociative 4-manifolds M_4 in (4.3) with the SO(3) symmetry, we need to fix the angular dependence as in (4.9) and allow more general radial dependence that will be encoded in a single function g of the radial variable $r = |\vec{x}|$. In particular, separating radial and angular variables, the equation for complex surface (4.9) can be written as

$$\vec{x} = \epsilon(\cosh \rho)\widehat{m} \,, \quad \vec{y} = \epsilon(\sinh \rho)\widehat{n} \,, \quad |\widehat{m}| = |\widehat{n}| = 1 \,, \quad \widehat{m} \cdot \widehat{n} = 0 \,. \tag{4.10}$$

Note, the locus of small constant ρ defines a circle bundle over $\Sigma = S^2$.

JHEP11(2020)033

Then, inspired by (4.9) and (4.10), we look for a coassociative 4-manifold M_4 of the form

$$\vec{y} = g(r)\widehat{n}(\theta,\phi,\psi)\,, \qquad \widehat{n}\cdot\widehat{n} = 1\,, \qquad \widehat{m}\cdot\widehat{n} = 0\,, \tag{4.11}$$

where $\widehat{m} = (\theta,\phi,\psi)$ denote the standard angle coordinates on S^3. In these coordinates, the explicit expression for 1-form χ compatible with our choice of the harmonic function (4.8) is $\chi = n\cos\theta d\phi$, and the Taub-NUT space is parametrized by the "polar" coordinates (r,θ,ϕ,ψ) instead of the original ones $(\vec{x},\widetilde{\psi})$. The angular coordinate ψ here is related to $\widetilde{\psi}$ in (4.5) by

$$\widetilde{\psi} = n\psi\,. \tag{4.12}$$

From the last two equations in (4.11) it follows that, for each given $\widehat{m}$, the unit vector $\widehat{n}$ takes values in a circle. In fact, here we are interested in a solution such that $\widehat{n}$ winds exactly once around this circle as ψ runs from 0 to 2π. Implementing this in our ansatz (4.11) and requiring that M_4 is calibrated with respect to (4.4)–(4.8), we obtain a single ordinary differential equation (ODE) for the function $g(r)$:

$$\frac{dg}{dr} = \frac{(2n+Br)g}{g^2-nr}\,. \tag{4.13}$$

In fact, as we explain momentarily, the specific value of B is irrelevant, as long as $B\neq 0$. It can be changed to any other value by rescaling r and g. Therefore, as far as the dependence on B is concerned, there are essentially two cases to consider: $B=0$ and $B\neq 0$.

The ordinary differential equation (4.13) is a special instance (with $A=4$) of a more general family of ODEs

$$\frac{dg}{dr} = \frac{(A+Br)g}{g^2-2r} \tag{4.14}$$

which are equivalent, via $f = \frac{1}{2}g^2 - r$, to the Abel equation of the second kind[7]

$$f\frac{df}{dr} = (A-1+Br)f + r(A+Br) \tag{4.15}$$

The substitution $z = \int(A-1+Br)dr$ brings it to the canonical form[8]

$$f\frac{df}{dz} = f + \Phi(z) \tag{4.16}$$

where $\Phi(z)$ is defined parametrically, by eliminating r in the relations

$$\Phi = \frac{Ar+Br^2}{A-1+Br}\,, \qquad z = (A-1)r + \frac{B}{2}r^2 + \text{const} \tag{4.17}$$

In analyzing the solutions of (4.13) and (4.14) it will be convenient to consider even a larger family of ODEs:

$$\frac{dg}{dr} = \frac{(A+Br)g}{g^2-2Cr} \tag{4.18}$$

[7] We thank Robert Bryant for pointing this out to us.

[8] Also note that, via a change of variable $F = f^{-1}$, we can bring (4.15) into the form of the Abel equation of the first kind:

$$\frac{dF}{dr} = -(A-1+Br)F^2 - r(A+Br)F^3\,.$$

JHEP11(2020)033

with three parameters, A, B and C. When parameters A and C are related as in (4.13), i.e. $A = 2n = 4C$, this more general ODE has a peculiar property that all parameters can be scaled away completely[9] by rescaling g and r,

$$g \;\to\; \lambda_g g\,, \qquad r \;\to\; \lambda_r r \tag{4.19}$$

In particular, when $B \neq 0$, without loss of generality we can bring it to a form (4.14) with $A = 4$ and $B = 1$.

Now, let us explore solutions to the above Abel equation, starting with the special ones that correspond to setting either A or B to zero. When $n = 0$, i.e. $A = C = 0$ in (4.18), a simple solution is

$$\text{NS5-brane}: \qquad g^2 - Br^2 = \text{const} \tag{4.20}$$

It describes the original NS5-brane (4.9) without D6 or D4-branes. Another special case corresponds to setting $B = 0$ in (4.14) and leads to a famous asymptotically conical coassociative submanifold in $\mathbb{R}^7$ constructed by Harvey and Lawson [18].

Indeed, after a change of variable $r = \rho^2/8$ our ODE with $B = 0$ has the property that both the numerator and denominator on the right-hand side are homogeneous (of degree 2) in g and ρ. As usual in such cases, the standard substitution $u = \frac{g}{\rho}$ gives

$$\frac{d\rho}{\rho} = \left(\frac{Au}{4u^2-1} - u\right)^{-1} du \tag{4.21}$$

and allows to write the explicit solution:

$$g\Big[(A+1)\rho^2 - 4g^2\Big]^{A/2} = \text{const} \tag{4.22}$$

The case $A = 4$ is precisely the solution of Harvey and Lawson:

$$M_4 = \Big\{\, (gqi\bar{q}, \rho\bar{q}) \in \operatorname{Im}\mathbb{H} \oplus \mathbb{H}\,, \quad q \in \mathrm{Sp}(1)\,, \quad g(4g^2 - 5\rho^2)^2 = \epsilon \,\Big\} \tag{4.23}$$

Topologically, this coassociative 4-manifold is a spin bundle over S^2. Therefore, as expected, our coassociative submanifolds defined by the ansatz (4.11) generalize the Harvey-Lawson construction by replacing $\mathbb{R}^7$ with a more general 7-manifold $X_7 = \mathbb{R}^3 \times \mathrm{TN}_n$.

4.1 Solving the Abel equation

Now, let us study solutions to (4.13) and (4.14) more systematically. Motivated by the special solutions (4.20) and (4.23) we first consider the behavior of g in the limits of small and large r.

[9] Specifically, under (4.19) this equation becomes

$$\frac{dg}{dr} = \frac{(4\lambda_g^{-2}\lambda_r C + B\lambda_g^{-2}\lambda_r^2 r)g}{g^2 - 2\lambda_g^{-2}\lambda_r C r}\,.$$

JHEP11(2020)033

Asymptotic behavior

Small r. In the limit $r \to 0$, the equation (4.14) can be approximated by

$$\frac{dg}{dr} = \frac{A\, g}{g^2 - 2r}, \tag{4.24}$$

whose solution is

$$r = \frac{g^2}{2 + 2A} + c_1\, g^{-2/A}, \tag{4.25}$$

where c_1 is an integration constant determined by the boundary conditions.

For concreteness, let us consider a *separatrix* solution that corresponds to the initial condition $g(0) = 0$, i.e. $c_1 = 0$. We thus get

$$g = \sqrt{(2 + 2A)r}. \tag{4.26}$$

Large r. Assuming that g grows faster than $r^{1/2}$ as $r \to \infty$, an assumption that we shortly verify to be self-consistent, (4.14) becomes:

$$\frac{dg}{dr} = \frac{r}{g}, \tag{4.27}$$

where we set $B = 1$ by scaling symmetries (4.19). The solution to this approximate equation is

$$g = \sqrt{r^2 + \zeta}. \tag{4.28}$$

If we are interested in the leading behavior at large r, the integration constant ζ can be neglected.

Full solution: the interpolating function

Let us introduce the following function

$$g_0 = \sqrt{(2 + 2A)r + r^2}, \tag{4.29}$$

which reproduces the small and large r asymptotic behavior of g. Figure 4 presents a comparison between the numerical solution for g and g_0 for $A = 1$. The two functions rapidly become indistinguishable for larger values of r. We will later discuss the accuracy of this approximation in further detail and its dependence on A.

It is convenient to decompose g into a product as follows

$$g = g_0 f, \tag{4.30}$$

where g_0 takes care of the asymptotic behavior as $r \to 0$ and ∞. We refer to f as the *interpolating function*. It is clearly a function with the boundary values $f(0) = f(\infty) = 1$. Plugging (4.30) into (4.14), we obtain the following differential equation for f

$$\frac{df}{dr} = \frac{f}{r}\left[\frac{(A + r)}{(2 + 2A + r)f^2 - 2} - \frac{(1 + A + r)}{(2 + 2A + r)}\right]. \tag{4.31}$$

JHEP11(2020)033

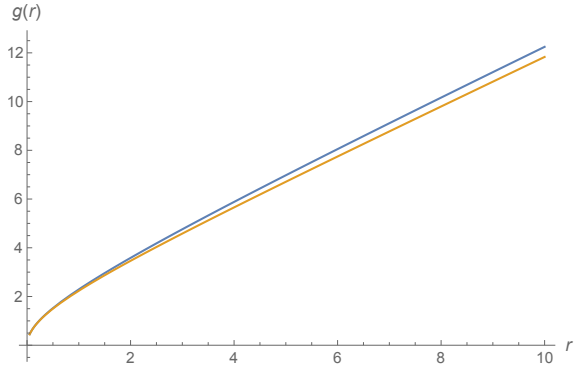

Figure 4. Comparison between the numerical solution for g (blue) and g_0 (orange) for $A = 1$.

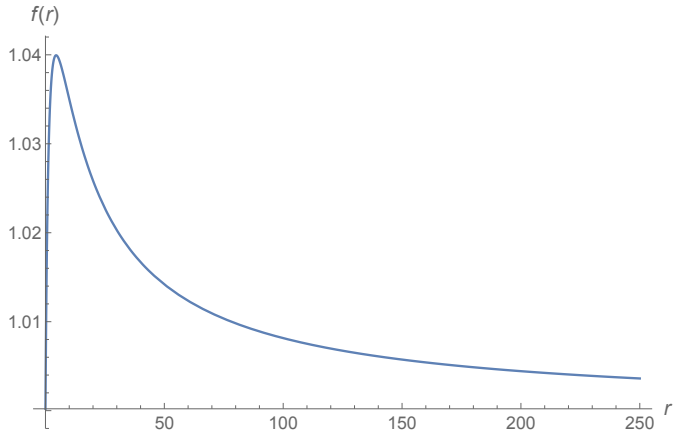

Figure 5. Numerical solution for the interpolating function f with $A = 1$.

The $A = 1$ case

Let us first consider the case of $A = 1$. Figure 5 shows the function f, obtained by numerically solving (4.31). It is interesting to note that the maximum value of f is around 1.04, which means that in this case g_0 is already a reasonably good approximation to g, differing from it by at most 4%.

This function becomes remarkably simple and suggestive when plotted in log-log scale, as shown in figure 6.

An approximate solution. Motivated by the simplicity of figure 6, we propose an analytical approximation f_{app} to f. This is given by the 4-parameter function

$$f_{\text{app}} = (1-\alpha) + \alpha\, e^{C\, e^{-\frac{(\log(r)-\log(r_0))^2}{2\Delta^2}}} . \tag{4.32}$$

Let us briefly motivate this expression. First of all, at $\alpha = 1$, it gives a Gaussian function in log-log scale, which is a natural ansatz in view of figure 6. To achieve a better fit, we introduced an additional parameter α. From the point of view of the second term, in log-log scale it would correspond to a vertical shift by $\log \alpha$. The first term guarantees that $f_{\text{app}}(0) = f_{\text{app}}(\infty) = 1$.

JHEP11(2020)033

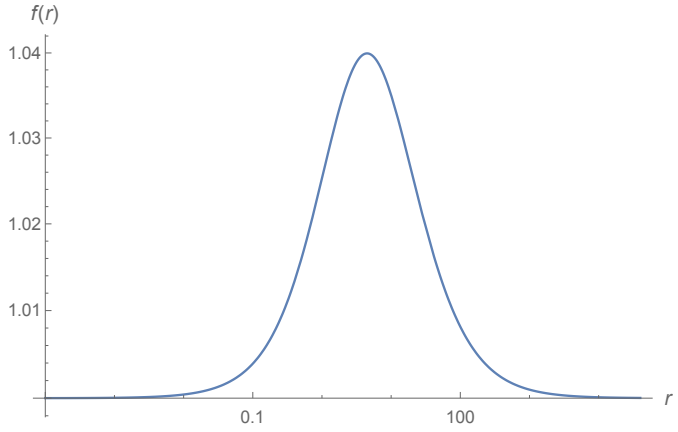

Figure 6. Log-log plot of the numerical solution for the interpolating function f with $A = 1$.

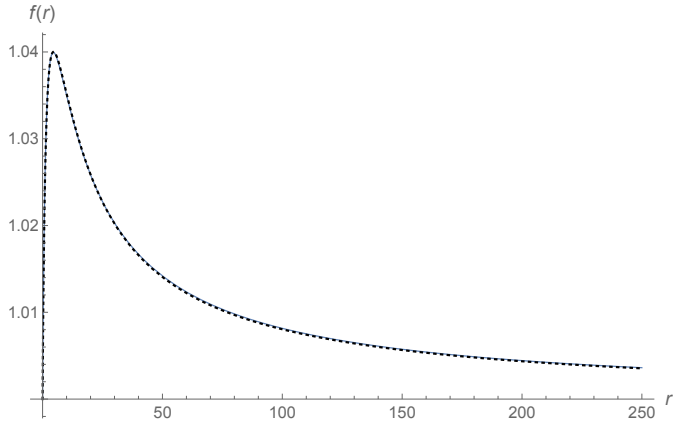

Figure 7. Comparison between the numerical solution for f (blue) and the fitted f_{app} (dotted) for $A = 1$.

Parameter fit. Figures 7 and 8 compare f to the best fit of the numerical solution by f_{app}. The fit was obtained by sampling the numerical solution at 500 points equally spaced in $\log r$, between $r = 10^{-5}$ and $r = 10^{5}$. Increasing the number of sample points does not noticeably modify the fit. The fitted parameters for this case are: $\alpha = 0.00726475$, $C = 1.87302$, $r_0 = 4.59284$, and $\Delta = 2.26916$.

The function (4.32) provides an excellent, albeit not perfect, fit to f. Indeed, it is possible to verify that there is no choice of parameters such that f_{app} is a solution of (4.31). It would be interesting to investigate whether a small modification of it yields an exact solution.

General A

We now consider the case of general A, including the value $A = 4$ of interest in (4.13). Since the analysis is identical to the one for $A = 1$, our presentation will be more succinct. Figure 9 shows f for various values of A ranging from 1 to 10, obtained by numerically solving (4.31). Once again, f becomes extremely simple in log-log scale, as shown in figure 10.

JHEP11(2020)033

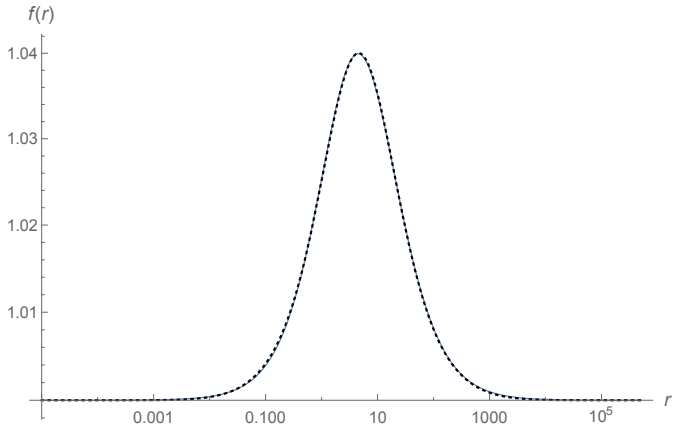

Figure 8. Log-log plot of the comparison between the numerical solution for f (blue) and the fitted f_{app} (dotted) at $A = 1$.

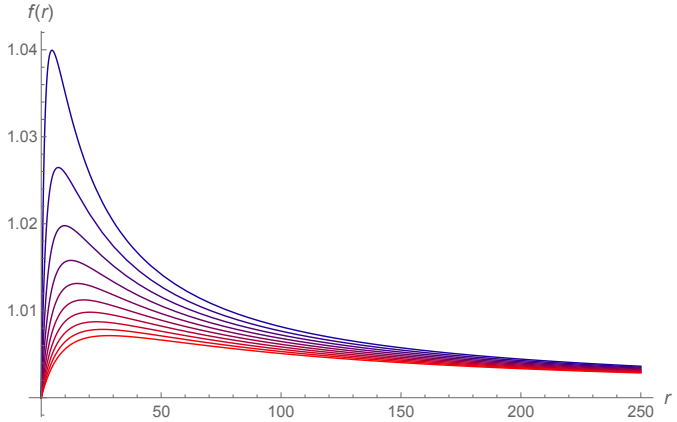

Figure 9. Numerical solution for f for $A = 1$ (blue) to $A = 10$ (red).

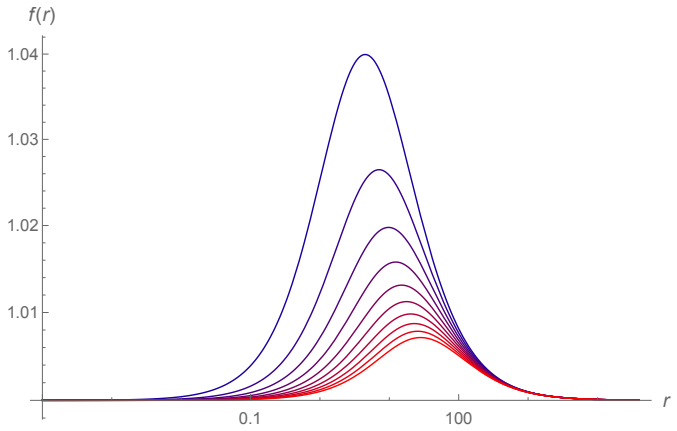

Figure 10. Log-log plot of the numerical solution for f for $A = 1$ (blue) to $A = 10$ (red).

JHEP11(2020)033

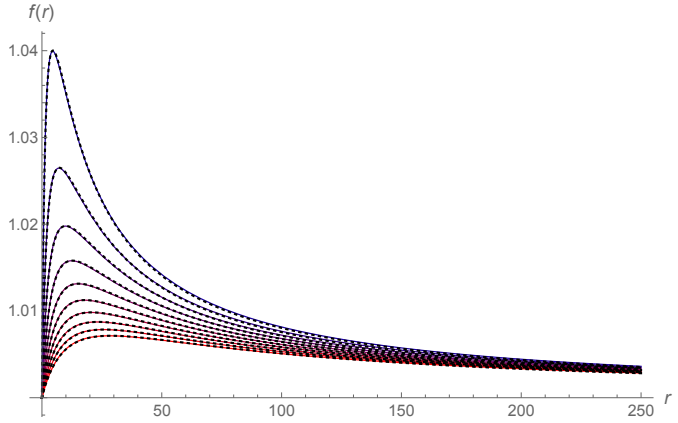

Figure 11. Comparison between f, for $A = 1$ (blue) to $A = 10$ (red), to the fitted f_{app} (dotted).

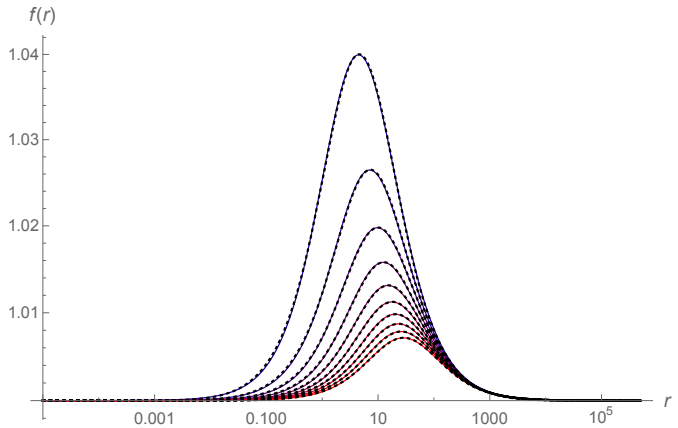

Figure 12. Log-log plot of the comparison between f, for $A = 1$ (blue) to $A = 10$ (red), to the fitted f_{app} (dotted).

Parameter fit. As in the case $A = 1$, f_{app} provides an excellent approximation to f for all A. Figures 11 and 12 compare f for values of A in the range $1, \ldots, 10$ to their fits by f_{app}. The parameters have been fitted using the same method as before. Below we present them for reference.

A	α	C	r_0	Δ
1	0.00726475	1.87302	4.59284	2.26916
2	0.00412429	2.00496	7.28069	2.28823
3	0.00286021	2.06973	9.97222	2.29881
4	0.00218574	2.1077	12.665	2.30526
5	0.00176766	2.13258	15.3582	2.30959
6	0.00148362	2.15003	18.0519	2.31264
7	0.00127792	2.16309	20.7456	2.31497
8	0.00112233	2.17309	23.4394	2.31675
9	0.00100046	2.18105	26.1333	2.31818
10	0.000902438	2.18753	28.8273	2.31934

(4.33)

JHEP11(2020)033

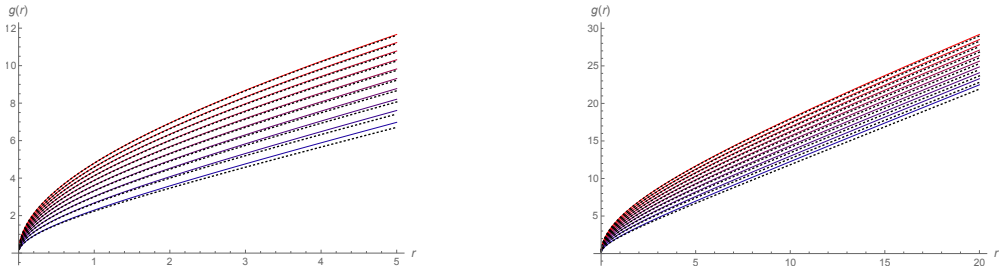

Figure 13. Comparison between g, for $A = 1$ (blue) to $A = 10$ (red), to g_0 (dotted). We consider the ranges: a) $0 \leq r \leq 5$ and b) $0 \leq r \leq 20$.

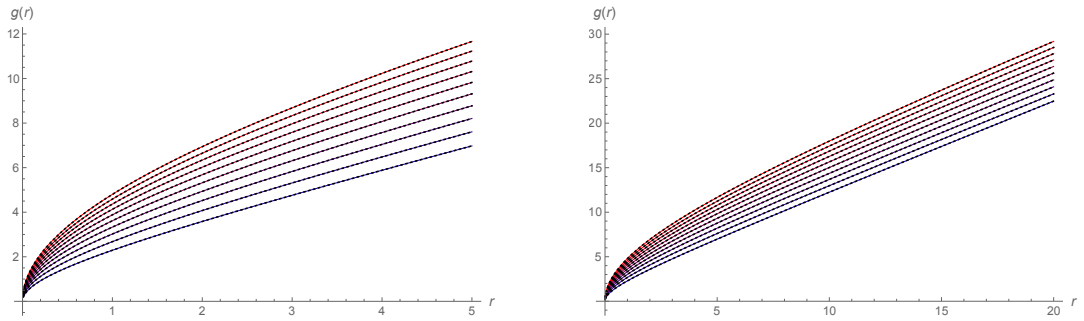

Figure 14. Comparison between g, for $A = 1$ (blue) to $A = 10$ (red), to $g_0 f_{\text{app}}$ (dotted). We consider the ranges: a) $0 \leq r \leq 5$ and b) $0 \leq r \leq 20$.

The full function

We are now ready to put together the asymptotic function g_0 with the analytic approximation to the interpolating function f_{app} and compare it to g.

Comparison to g_0. In order to appreciate how things improve by introducing f_{app}, it is convenient to first compare g to g_0, as shown in figure 13. We show two ranges of small r, that is where the deviations are most noticeable. We see that g_0 becomes a better approximation to g as A increases. We will revisit this observation shortly.

Comparison to $g_0 f_{\text{app}}$. Figure 14 compares g to the analytic approximation given by $g_0 f_{\text{app}}$ for $A = 1, \ldots, 10$. The functions become indistinguishable to a naked eye.

The $A \to \infty$ limit

Figures 9 and 10 show that the maximum value of f decreases as A grows. In other words, g_0 becomes a better approximation to g as A is increased. The maximum discrepancy between the two functions goes from 4% for $A = 1$ to 0.7% for $A = 10$. For $A = 40$ this number reduces to 0.2%.

We can discuss this behavior in terms of f_{app}, since it gives a good approximation to f. The maximum of f_{app} is $f_{\text{app}}(r_0) = 1 + \alpha(e^B - 1)$. Computing the fits up to $A = 40$, we observe that B seems to converge to a finite value while α appears to decrease to zero. This leads us to conjecture that $f_{\text{app}} \to 1$ as $A \to \infty$ or, equivalently, that g_0 becomes the

JHEP11(2020)033

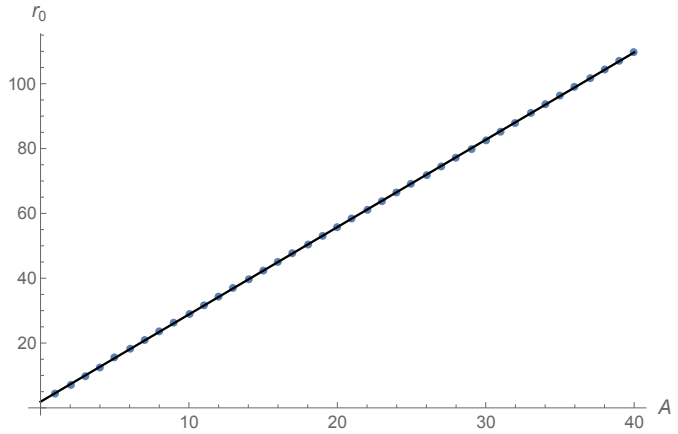

Figure 15. Value of r_0 as a function of A up to 40 and its linear fit.

exact solution in the $A \to \infty$ limit. Notice that this is not just the small r solution (4.26), since for sufficiently large r the behavior of g is controlled by B.

We can offer more details on how this limit is approached. The interpolating function f accounts for the transition between the small and large r regimes of g. The value of r_0 is a natural indicator of where this transition occurs. Interestingly, r_0 depends linearly on A, as shown in figure 15. As A grows, not only $f_{\rm app}$ approaches 1, signaling that g_0 becomes a better approximation to g, but also r_0 grows, indicating that the small r approximation is valid up to larger values of r, as expected.

L^2 norms

For the Harvey-Lawson solution (4.23), it was shown in [10] that the deformation mode ϵ is not L^2 normalizable:

$$\int_{M_4} d^4x \sqrt{\det(g_{\mu\nu} + \delta g_{\mu\nu})} - \int_{M_4} d^4x \sqrt{\det(g_{\mu\nu})} \;\to\; \infty \tag{4.34}$$

For $B = 0$ and more general (integer) values of A, from (4.22) we find

$$\frac{\delta g}{\delta \epsilon} = \frac{1}{(A+1)(\rho^2 - 4g^2)} \left(\frac{g}{\epsilon}\right)^{\frac{A-2}{A}} \sim \rho^{-\frac{A+2}{A}} \qquad \text{as} \quad \rho \to \infty \tag{4.35}$$

This exhibits a faster than ρ^{-2} decay when $A < 2$, which is the condition for the deformation mode ϵ to be L^2 normalizable. If $A > 2$, the ϵ-mode is not L^2 normalizable and usually this means that it should be interpreted as a parameter (coupling constant) of the IR theory, rather than a dynamical field with finite kinetic term.

In our present context the IR theory is a two-dimensional $\mathcal{N} = (0, 2)$ theory that "lives" on the $\mathbb{R}^2$ part of the fivebrane world-volume (1.8). As is well known, in two space-time dimensions, long range quantum fluctuations do not allow fixing vacuum expectation values, and so all moduli tend to be dynamical. Therefore, the fact that ϵ mode is not L^2 normalizable reinforces the conclusion that it should be interpreted as a coupling constant

JHEP11(2020)033

rather than a vev of a dynamical field. Another closely related aspect is whether a singularity $\epsilon = 0$ occurs at finite distance in the moduli space metric, see e.g. [21] for a close cousin of our problem where "compactification" on a non-compact 4-manifold is replaced by a "compactification" on a non-compact Calabi-Yau 4-fold.

One possible modification of the estimate (4.35) can be due to the fact that it was deduced under the assumption $B = 0$. Indeed, as we noted several times earlier, the large-r behavior of the solution is controlled entirely by B, not A. Thanks to the detailed analysis in this section, however, it is easy to see that incorporating $B \neq 0$ still leads to the same conclusion as (4.35). Namely, from (4.29)–(4.30) and (4.32) we quickly find the large-r behavior of $g \sim r$ and $\frac{\delta g}{\delta \zeta} \sim r^{-1}$, which means that the deformation mode is not L^2 normalizable.

4.2 Reversing the degree

The differential equation (4.13) and its solutions described above correspond to D4-NS5 brane models with non-compact D4-branes of the form (3.16). Moreover, as explained in the end of section 3, brane models with compactly supported D4-branes, as in (2.3), differ by the orientation reversal on the fibers of X_7 or, equivalently, $n \to -n$.

In our parametrization of the coassociative submanifolds (4.11), this corresponds to simultaneously changing the sign of g and r. Therefore, the corresponding version of the ODE (4.13) reads ($n > 0$)

$$\frac{dg}{dr} = \frac{(-n + |n| + Br)g}{g^2 + nr} = \frac{Brg}{g^2 + nr}\,. \tag{4.36}$$

The term $|n|$ is not affected by the sign flip, cancels against $(-n)$, and leads to the main qualitative difference between (4.13) and (4.36). The $|n|$ term is needed to maintain the components of Taub-NUT metric positive. One important consequence is that, although the resulting configuration is free of the winding number anomaly, it breaks supersymmetry and hence is likely to be unstable.

In figure 16, we plot a numerical solution to the differential equation (4.36) with $B = 1$. For comparison, we also plot a numerical solution to the differential equation (4.13) with $B = 1$. Note that the SO(3)-rotation (4.10)–(4.11) of the graph of function $g(r)$ discussed earlier in this section produces coassociative submanifolds that correspond to NS5-D4 brane systems with non-compact D4-branes on "disk complements" (3.16). A similar SO(3)-rotation of the graph of function $g(r)$ presented in the first plot of figure 16 clearly has only one asymptotic region $\cong \mathbb{R}_+ \times S^3/Z_n$ that corresponds to M-theory lift of NS5-branes and, therefore, D4-branes in this brane model are compactly supported on Lagrangian disks (2.3).

In summary, we have found two types of differential equations, both free of Euler number anomaly. The first type (4.13) preserves supersymmetry and describes a disk complement. The second type (4.36) breaks supersymmetry and describes a compact disk. It would be interesting to include both the D4 disk and the D4 disk complement touching each other through the NS5-brane at a non-zero angle. Such configurations supported bi-fundamental matter fields in brane-brick models [4].

JHEP11(2020)033

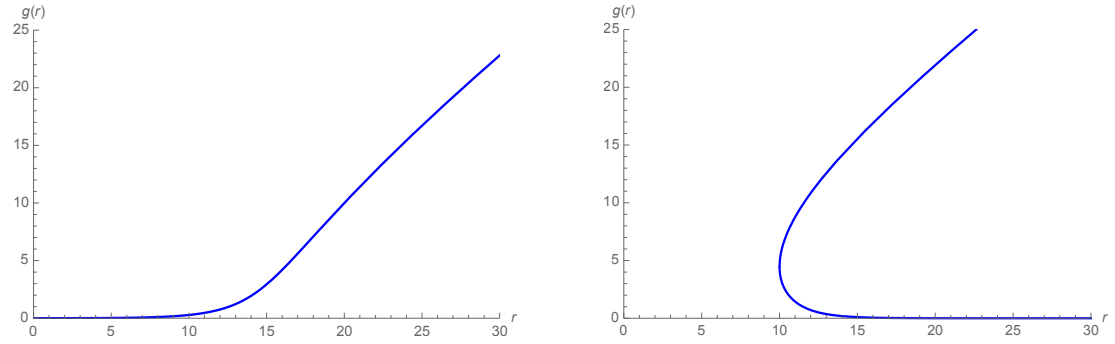

Figure 16. (left) a numerical solution to the differential equation (4.36), (right) a numerical solution to the differential equation (4.13).

5 Phase transitions and Spin(7) manifolds

In the previous section, we constructed new coassociative submanifolds $M_4 \subset X_7 = \Lambda^{2,+}(\mathrm{TN}_n)$ of topology $L(n,1)\times\mathbb{R}$, or TN_n, or $\mathcal{O}(n)\to\mathbb{C}\mathbf{P}^1$, or any combinations thereof. These are particular examples of a more general construction (3.15), which can be carried out in detail following the steps of section 4.

As explained in the Introduction, every such pair (M_4, X_7) determines a manifold X_8 of Spin(7) holonomy that, in physics, arises from an (auxiliary) problem of D6-branes supported on $\mathbb{R}^3\times M_4$. The topology of X_8 is determined by the topology of M_4 and X_7. Specifically, X_8 is the total space of a circle bundle over X_7 with a codimension-4 singular locus $M_4\subset X_7\cong X_8/S^1$. (Note, codimension of the singular locus is always even, and must be equal to 4 in order for the fibration to be smooth.) In our class of examples, this means that the space of Spin(7) holonomy metrics consists of several branches (or phases).

Indeed, consider, for concreteness, the case of $n=1$. Then, one choice of the coassociative submanifold M_4 is a disjoint union of a Taub-NUT space TN_1 and $\mathcal{O}(+1)\to\mathbb{C}\mathbf{P}^1$:

$$\text{Phase A:}\qquad M_4 \;=\; \begin{array}{c}\mathcal{O}(+1)\\ \downarrow\\ \mathbb{C}\mathbf{P}^1\end{array} \;\bigsqcup\; \text{Taub-NUT} \tag{5.1}$$

In this phase, the corresponding S^1-fibration has topology[10] $X_8^{(A)}\cong\mathbb{R}^4\times\mathbb{C}\mathbf{P}^2$ and depends on one real deformation parameter that we can choose to be $\mathrm{Vol}(\mathbb{C}\mathbf{P}^2)$. As $\mathrm{Vol}(\mathbb{C}\mathbf{P}^2)\to 0$, the Spin(7) holonomy metric on $X_8^{(A)}$ develops an isolated conical singularity which, aside from $X_8^{(A)}$, admits another resolution ("desingularization") by a family of Spin(7) holonomy metrics on $X_8^{(B)}\cong\mathbb{R}^3\times S^5$. This family of Ricci-flat metrics, conjectured in [10] and only recently constructed in [22], can also be obtained as the total space of a circle bundle over the same X_7, but with a different locus of singular S^1 fibers

$$\text{Phase B:}\qquad M_4 = S^3\times\mathbb{R} \tag{5.2}$$

[10]Sometimes we write non-trivial vector bundles simply as products (or, more precisely, our use of "$\cong$" means homotopy eqivalence). For example, $X_8^{(A)}$ here is the total space of the universal quotient bundle over $\mathbb{C}\mathbf{P}^2$.

JHEP11(2020)033

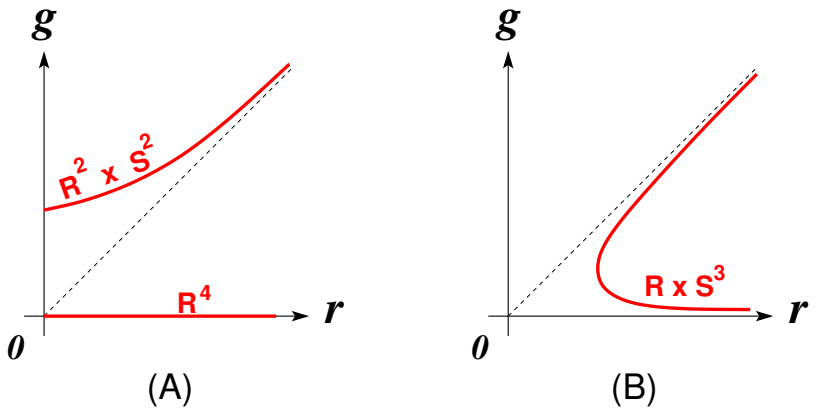

Figure 17. Two geometric phases of the coassociative 4-manifold (5.1)–(5.2) in $\mathbb{R}^3 \times$ Taub-NUT. To illustrate only the homotopy type, we replace Taub-NUT by $\mathbb{R}^4$ and Spin bundle over $\mathbb{C}\mathbf{P}^1 \cong S^2$ by $\mathbb{R}^2 \times S^2$.

The topology changing transition between these two coassociative submanifolds — or, between the corresponding Spin(7) manifolds $X_8^{(A)}$ and $X_8^{(B)}$ — passes through the singular geometry, for which M_4 is a cone on $S^3 \sqcup S^3$.

A natural question, then, is: What is the physics of this transition? From the M-theory viewpoint, it requires studying the effective 3d $\mathcal{N} = 1$ theory obtained by compactification on X_8. From the perspective of type IIA theory on X_7, it requires understanding world-volume theory of the D6-brane supported on $\mathbb{R}^3 \times M_4$. Either way, the result of this analysis is a simple 3d $\mathcal{N} = 1$ theory [10]:

$$\text{U}(1) \text{ gauge theory a } \mathcal{N} = 1 \text{ matter multiplet of charge } +1$$

such that what we call phase A and phase B correspond to Higgs and Coulomb branches of this effective theory. In fact, a notable feature of this effective theory is that it has two components of the Higgs branch on which the parity symmetry of the three-dimensional theory is spontaneously broken by the half-integer Chern-Simons term, $k_{\text{eff}} = +\frac{1}{2}$ and $k_{\text{eff}} = -\frac{1}{2}$. In the world-volume theory of the D6-brane, these Chern-Simons couplings originate from the flux quantization condition [23]:

$$\int_{\mathbb{C}\mathbf{P}^1} \frac{F}{2\pi} = k \in \mathbb{Z} + \frac{1}{2} \tag{5.3}$$

and the fact that $\mathcal{O}(+1) \to \mathbb{C}\mathbf{P}^1$ is not Spin.

2d phase transitions for $n = 1$

Naively, one might expect that the effective 2d $\mathcal{N} = (0, 2)$ theory on the fivebrane world-volume in our setup (1.8) is similar to the effective theory of a D6-brane compactified on the same coassociative 4-manifold. In particular, for the two choices (5.1)–(5.2) of M_4, with $n = 1$, one might expect two phases, which we still continue calling phase A and phase B.

JHEP11(2020)033

phase	X_8	M_4	3d phase	parity	$\mathrm{U}(1)_J$
A	$\mathbb{R}^4 \times \mathbb{C}\mathbf{P}^2$	$\mathbb{R}^2 \times S^2 \sqcup \mathbb{R}^4$	Higgs	✗	✓
B	$\mathbb{R}^3 \times S^5$	$S^3 \times \mathbb{R}$	Coulomb	✓	✗

Table 1. Two geometric phases of Spin(7) holonomy manifolds X_8 correspond to Higgs and Coulomb phases of 3d $\mathcal{N} = 1$ effective field theory.

However, looking into the analysis a little more closely one quickly runs into questions, which indicate that the physics of M5-branes can be rather different from the physics of D-branes, even when they wrap the same coassociative submanifolds. For example, one question about the fivebrane system (1.8) is: What is the analogue of the Freed-Witten anomaly (5.3)? And, does it lead to two vacua in phase (5.1)?

Since the world-volume theory of a single fivebrane has a Lagrangian description, one might hope to deduce the effective 2d $\mathcal{N} = (0, 2)$ theory simply by following the standard rules of the Kaluza-Klein reduction. However, by looking at the KK spectrum in [24], it is not immediately clear what the answer should be for $M_4 = S^3 \times \mathbb{R}$. This manifold has no homology in degrees up to 3, whereas all fields of 6d $(0, 2)$ theory on the fivebrane world-volume are represented by differential forms of degree less than 3, even after the partial topological twist along M_4. So, naively, the resulting 2d $\mathcal{N} = (0, 2)$ theory looks completely empty in phase (5.2). Another issue is that $M_4 = S^3 \times \mathbb{R}$ is non-compact, whereas the Kaluza-Klein spectrum summarized in table 1 of [24] assumes compactness of M_4. So, how shall we even think of this compactification from 6d to 2d on a non-compact M_4?

Another puzzle has to do with the fact that, in M-theory compactification on Spin(7) manifold $X_8^{(B)} \cong \mathbb{R}^3 \times S^5$ a key role is played by the charged particle coming from M5-brane wrapped on the 5-sphere S^5. In the corresponding type IIA setup with a D6-brane supported on a coassociative 4-manifold $M_4 = S^3 \times \mathbb{R}$, this charged particle comes from a D4-brane with world-volume $\mathbb{R} \times D^4$, such that $\partial D^4 = S^3$. But, what is the corresponding analogue of this charged state in a setup with M5-branes on the same coassociative manifold $M_4 = S^3 \times \mathbb{R}$? The only candidate could be an M2-brane ending on the M5-brane, but the dimension of M2-brane world-volume is too small for this. On the other hand, in a different phase, where $M_4 \cong \mathbb{R}^2 \times S^2$, M2-branes supported on D^3 and ending on M5-brane along the $S^2 = \partial D^3$ produce instantons (local operators) in 2d $(0, 2)$ theory. What is their role?

Luckily, all these questions conveniently resolve one another. For example, in the case of 3d $\mathcal{N} = 1$ phases, the spontaneous symmetry breaking in phase A that leads to two vacua with $k = +\frac{1}{2}$ and $k = -\frac{1}{2}$ is accompanied by the existence of a domain wall that interpolates between these vacua. In M-theory on $\mathbb{R}^3 \times X_8^{(A)}$, this half-BPS domain wall is a M5-brane supported on $\mathbb{R}^2 \times \mathbb{C}\mathbf{P}^2$, such that $\mathbb{R}^2 \subset \mathbb{R}^3$ and $\mathbb{C}\mathbf{P}^2 \subset X_8^{(A)}$ is a topologically non-trivial calibrated (Cayley) 4-cycle. In the corresponding type IIA setup with a D6-brane supported on $\mathbb{R}^3 \times M_4$, this half-BPS domain wall is a D4-brane with world-volume $\mathbb{R}^2 \times D^3$, such that $\mathbb{R}^2 \subset D^3$ as before, and $\partial D^3 = S^2 \subset M^4$ is a topologically non-trivial 2-cycle.

Since, upon reduction on S^1, the 2-form field on fivebrane world-volume gives rise to a gauge field 1-form on D4-brane world-volume, one might expect that anomalous quan-

JHEP11(2020)033

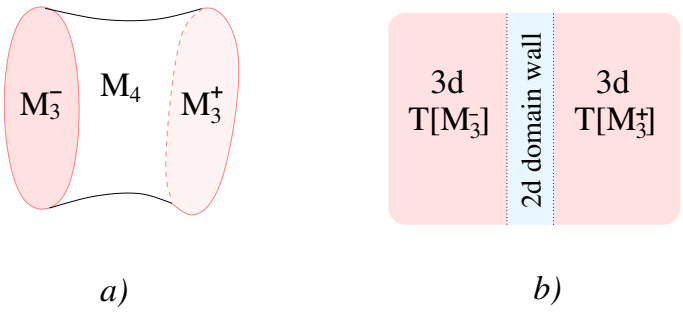

Figure 18. (a) A cobordism between 3-manifolds M_3^- and M_3^+ corresponds to (b) a 2d $\mathcal{N} = (0, 2)$ theory $T[M_4]$ on the domain wall (interface) coupled to 3d $\mathcal{N} = 2$ theories $T[M_3^-]$ and $T[M_3^+]$ on both sides [15].

tization condition (5.3) on D4-brane world-volume comes from a similar anomaly for the 2-form. Moreover, one would also expect that, in case of M5-branes, this anomaly is responsible for spontaneous breaking of 1-form symmetry, since after compactification on S^1 it becomes the origin of a spontaneous breaking of ordinary symmetry on D4-brane theory. Both of these expectations are, in fact, correct, cf. [15, 25].

Indeed, just like ordinary symmetry breaking is accompanied by the existence of domain walls that interpolate between vacua (in our case, labeled by $k = +\frac{1}{2}$ and $k = -\frac{1}{2}$), 1-form symmetry breaking is accompanied by codimension-2 vortices. In our fivebrane setup (1.8), these half-BPS vortices are precisely M2-branes supported on $\{\text{pt}\} \times D^3$ that were mentioned in one of the above questions. Note, that these M2-brane vortices only exist in phase (5.1), same geometric phase that hosts half-BPS domain walls in 3d $\mathcal{N} = 1$ theory and has $w_2(M_4) \neq 0$.

Now let us address non-compactness of M_4, which also quickly turns on its head from an ugly problem into a nice feature. Indeed, since both choices of M_4 in phases (5.1) and (5.2) are non-compact, with two asymptotic regions $\approx \mathbb{R} \times S^3$, we should really think of these 4-manifolds as cobordisms from $M_3^- \cong S^3$ to $M_3^+ \cong S^3$. A "compactification" of a fivebrane on such cobordisms has a simple interpretation as an interface[11] between 3d $\mathcal{N} = 2$ theories $T[M_3^-]$ and $T[M_3^+]$, illustrated in figure 18.

Since $M_3^+ \cong M_3^-$, in our present problem we have the same theory $T[M_3^\pm]$ on both sides of the interface. In fact, we already encountered this 3d $\mathcal{N} = 2$ theory for general value of n in our previous discussion, cf. (3.11). Here we need its version with $n = 1$ and $G = \mathrm{U}(1)$, that is a U(1) super-Chern-Simons theory at level 1 with an additional 3d $\mathcal{N} = 2$ free chiral multiplet. Therefore, it remains to identify two 2d $\mathcal{N} = (0, 2)$ interfaces in this theory, which correspond to (5.1) and (5.2), respectively (or, more precisely, two phases of the *same* interface related by a 2d phase transition).

In one of these cases, the answer is simple: namely, in phase (5.2) the interface is "trivial" or "fully transparent." Concretely, this means that it identifies the $\mathrm{U}(1)_+$ and $\mathrm{U}(1)_-$ gauge multiplets of theories $T[M_3^+]$ and $T[M_3^-]$, as well as free chiral multiplets on

[11] equivalently, a non-dynamical domain wall.

JHEP11(2020)033

both sides. Note, in the 2d $\mathcal{N} = (0, 2)$ theory on the interface, $\mathrm{U}(1)_+$ and $\mathrm{U}(1)_-$ appear as global symmetries.

The phase A of our 2d interface is more interesting. (Recall, that the bulk 3d theory does not change, and it is only the 2d interface that undergoes a phase transition.) In this phase, our 2d interface is geometrically "engineered" by a compactification of 6d fivebrane theory on a 4-manifold with two connected componets,

$$M_4 = M_4^- \sqcup M_4^+ \tag{5.4}$$

where, according to (5.1),

$$M_4^- = \begin{array}{c} \mathcal{O}(+n) \\ \downarrow \\ \mathbb{C}\mathbf{P}^1 \end{array}, \qquad M_4^+ = \mathrm{TN}_n \tag{5.5}$$

written here, for convenience,[12] with general value of n. Each of these components has one asymptotic region of the form $\mathbb{R} \times S^3$, which corresponds to either left or right side of figure 18:

$$\partial M_4^\pm = M_3^\pm \quad \big(\cong S^3\big) \tag{5.6}$$

In other words, as our notations suggest, $T[M_4^+]$ couples to $T[M_3^+]$ and $T[M_4^-]$ couples to $T[M_3^-]$. Moreover, because the components of $M_4 = M_4^- \sqcup M_4^+$ are disjoint — in fact, separated by a distance controlled by the parameter $\epsilon \sim \mathrm{Vol}\big(S^2\big)$, cf. (2.1) — the two "halves" of the interface, $T[M_4^+]$ and $T[M_4^-]$, become weakly interacting (decoupled) as $\epsilon \to \infty$.

To summarize so far, our 2d interface $\mathcal{I}$ has two branches, geometrically engineered by topological reduction on (5.1) and (5.2). These branches are parametrized by $\mathrm{Vol}(S^2)$ and $\mathrm{Vol}(S^3)$, respectively. And, asymptotically, in the large volume limits, the interface becomes either fully transmissive or totally reflective, cf. [15]:

$$\begin{array}{lll} \text{Phase A:} & \text{Maximally reflective } \mathcal{I} = T[M_4^+] \otimes T[M_4^-] & \text{as } \mathrm{Vol}(S^2) \to \infty \\ \text{Phase B:} & \text{Identity interface } \mathcal{I} = \mathbf{1} & \text{as } \mathrm{Vol}(S^3) \to \infty \end{array} \tag{5.7}$$

Moreover, since for our choices of $M_4^\pm$ the individual 2d $\mathcal{N} = (0, 2)$ boundary theories $T[M_4^\pm]$ are known, it only remains to couple them in a consistent way, so that the combined 2d theory has two branches with the desired asymptotic behavior (5.7).

In phase A, the free chiral multiplet of 3d $\mathcal{N} = 2$ theory has Neumann boundary conditions on both sides of the interface, in $T[M_4^+]$ as well as in $T[M_4^-]$, meaning that in a decomposition to 2d $\mathcal{N} = (0, 2)$ chiral and Fermi multiplets the Fermi gets Dirichlet boundary conditions while the chiral obeys Neumann boundary conditions. A simple way

[12] For the arguments to follow, it will be important to pay careful attention to orientations, which is easier if we restore general n for a moment. As explained in [15], the manifolds A_{n-1} and $\mathcal{O}(-n) \to \mathbb{C}\mathbf{P}^1$ have oppositely oriented boundaries and unique Spin structures. Therefore, they can be glued to form a closed 4-manifold which, however, is not Spin. In our case, M_4^+ and M_4^- should be oriented in a way that allows a topology changing transition to $M_4 = \mathbb{R} \times L(n, 1)$. This means if $M_4^+ = A_{n-1}$, then M_4^- must be $\mathcal{O}(+n) \to \mathbb{C}\mathbf{P}^1$.

JHEP11(2020)033

to see this is to note that, in our general setup (1.8), each connected components of the M5-brane can move independently in the directions of $\mathbb{R}^4$ that are orthogonal to $\mathbb{R}^2$. For concreteness, we choose these directions to be x^3 and x^4.

In our present example (5.1), the fivebrane has two connected components, M_4^+ and M_4^-, and therefore the corresponding 2d effective theories $T[M_4^+]$ and $T[M_4^-]$ each come equipped with a "center of mass" $(0,2)$ chiral multiplet [24], whose (complex) scalar component parametrizes the motion along $x^3 + ix^4$. Naturally, we denote these two $(0,2)$ chiral multiplets in $T[M_4^+]$ and $T[M_4^-]$, respectively, by Φ_+ and Φ_-. These are precisely the restrictions (boundary values) of 3d $\mathcal{N} = 2$ chiral multiplet Φ_{3d} to the left and right boundaries of the 2d $\mathcal{N} = (0,2)$ interface:

$$\Phi_+ = \Phi_{3d}\big|_{\partial_+}\,, \qquad\qquad \Phi_- = \Phi_{3d}\big|_{\partial_-} \tag{5.8}$$

Note, in phase A, these two $(0,2)$ chiral multiplets are independent, whereas in phase B they are identified, cf. (5.7):

$$\begin{aligned} &\text{Phase A:} \quad \Phi_+ - \Phi_- = \epsilon = \mathrm{Vol}(S^2) \cdot \exp \int\limits_{S^2} B \\ &\text{Phase B:} \quad \Phi_+ = \Phi_- \end{aligned} \tag{5.9}$$

Here, through a minor abuse of notations, in phase A we also identified the difference of complex scalars in Φ_+ and Φ_- with the geometric parameters of the compactification on (5.1). In particular, B denotes the 2-form field[13] in 6d $(0,2)$ fivebrane theory

Note, the scalar fields in $T[M_4^+]$ and $T[M_4^-]$ parametrizing the motion in directions transverse to $\mathbb{R}^2 \subset \mathbb{R}^4$ can only be components of 2d $(0,2)$ chiral multiplets, which gives an *a priori* reason for (5.8) and for why the volume of $S^2 \subset M_4^-$ is complexified in (5.9). The rotation in these directions, that is directions we chose to call (x^3, x^4), is precisely the R-symmetry of 2d $\mathcal{N} = (0,2)$ boundary supersymmetry algebra on the interface:

$$\mathrm{U}(1)_R = \mathrm{U}(1)_{34} \tag{5.10}$$

In fact, for our M_4^+ and M_4^- as in (5.5), we know the complete description of the boundary theories $T[M_4^+]$ and $T[M_4^-]$, not just the sectors involving $(0,2)$ chiral fields $\Phi_\pm$. One of them, namely $T[M_4^+]$, we already encountered in section 3 when we introduced D6-branes in (3.12). In fact, this is precisely how M_4^+ in our example, given by (3.15), ended up being the Taub-NUT space. And, the reason for incorporating D6-branes and modifying (1.9) into (3.15) was to introduce chiral fermions charged under the gauge symmetry of 3d $\mathcal{N} = 2$ theory so as to cancel the anomaly. Therefore, according to that discussion, the 2d $\mathcal{N} = (0,2)$ theory $T[M_4^+]$ in our example is the simplest theory of a D4-D6 brane intersection. In general, such intersection of N D4-branes with n D6-branes supports nN Dirac fermions — i.e. nN Fermi multiplets in 2d $\mathcal{N} = (0,2)$ language — that transform in a bifundamental representation of $\mathrm{U}(n) \times \mathrm{U}(N)$, cf. [26].

From the viewpoint of 3d $\mathcal{N} = 2$ theory (3.11), this $T[M_4^+]$ imposes a Dirichlet boundary condition on the $G = \mathrm{U}(N)$ gauge field, whose "edge modes" (free Dirac fermions) realize $\mathrm{SU}(n)$ current algebra at level N. This can be also seen directly from the physics of the

[13] whose field strength is self-dual.

JHEP11(2020)033

6d fivebrane theory on $M_4^+ = \mathrm{TN}_n$, since $H^2(\mathrm{TN}_n, \mathbb{Z})$ is the root lattice of $A_{n-1} = \mathrm{SU}(n)$ and supports n harmonic L^2-normalizable 2-forms. These 2-forms are all anti-self-dual, which means [24] that the corresponding Kaluza-Klein modes belong to the left-moving (non-supersymmetric) sector of the 2d $\mathcal{N} = (0,2)$ theory $T[M_4^+]$. For our application, we are interested in the simplest case of this scenario, when $n = N = 1$, so that the edge modes consist of only one Dirac fermion, a 2d $\mathcal{N} = (0,2)$ Fermi multiplet that we call Ψ_+.

Similarly, $T[M_4^-]$ with M_4^- as in (5.5) is also fairly well understood; it plays an important role in gluing operations on 4-manifolds and the corresponding chiral algebras. Since M_4^- has positive-definite intersection form, we expect that edge modes should be represented by charged $(0,2)$ chiral multiplets, instead of Fermi multiplets that one has in a negative-definite case. This is indeed the case [24], and from the direct Kaluza-Klein reduction in our example we find that $T[M_4^-]$ carries a $(0,2)$ chiral multiplet P_- charged under the gauge symmetry $\mathrm{U}(1)_-$ of the 3d $\mathcal{N} = 2$ theory.[14] In the non-abelian case, that is for $N > 1$, the boundary theory $T[M_4^-]$ is more interesting and carries the left-moving algebra called $\overline{\mathcal{U}}$, see [27] for details.

Note, in the abelian case (that is, for $N = 1$), the bulk 3d theory $T[M_3^+] \cong T[M_3^-]$ has no fermions charged under the corresponding gauge symmetry $\mathrm{U}(1)_+$ or $\mathrm{U}(1)_-$. Therefore, the only contribution to the 2d chiral anomaly from 3d bulk comes from the Chern-Simons term, which contributes $\pm n$ to the 't Hooft anomaly of $T[M_4^\pm]$. The sign of the anomaly is opposite for the two sides of the interface since reversing the orientation is equivalent to reversing the sign of the Chern-Simons term. These two contributions $+1$ and -1 from the 3d Chern-Simons coupling are neatly canceled by the anomalies of 2d $(0,2)$ multiplets Ψ_+ and P_- charged under $\mathrm{U}(1)_+$ and $\mathrm{U}(1)_-$, respectively. In particular, the net anomaly is zero, which is crucial for the interface to become a trivial (identity) interface in phase B, where $\mathrm{U}(1)_+ = \mathrm{U}(1)_-$ becomes the gauge symmetry of the original 3d $\mathcal{N} = 2$ theory (3.11).

The last ingredient we need is a field whose scalar component can be identified with the volume of S^3 in phase (5.2). Since 2d $\mathcal{N} = (0,2)$ requires all scalars come in complex pairs, we propose that $\mathrm{Vol}(S^3)$ is a (real) part of a 2d $\mathcal{N} = (2,2)$ chiral multiplet, that is a pair of $(0,2)$ chiral and Fermi (Φ_0, Ψ_0):

$$\Phi_0 = \mathrm{Vol}(S^3) \cdot e^{i\theta} \tag{5.11}$$

Now we finally accounted for all key elements of the sought after 2d $\mathcal{N} = (0,2)$ theory with phases (5.7). Namely, it has two coupled sectors, $T[M_4^+]$ and $T[M_4^-]$, that correspond to the two sides of the interface in figure 18. The field content of $T[M_4^+]$ includes a Fermi multiplet Ψ_+ and a $(0,2)$ chiral multiplet Φ_+, whereas that of $T[M_4^-]$ contains two $(0,2)$ chiral multiplets Φ_- and P_-:

	Φ_+	Ψ_+	Φ_-	P_-	Φ_0	Ψ_0
$\mathrm{U}(1)_+$	0	+1	0	0	0	0
$\mathrm{U}(1)_-$	0	0	0	−1	0	0

(5.12)

[14] This switch from Fermi to chiral multiplets, and vice versa, is very typical under a parity reversal in 3d $\mathcal{N} = 2$ theory [15] or under orientation reversal on the 4-manifold [27].

JHEP11(2020)033

There is an obvious candidate for the supersymmetric interaction of these fields, namely a J-term superpotential, that leads to the desired vacuum structure (5.7):

$$\int d\theta^+ \, \Phi_0 P_- \Psi_+ \big|_{\bar\theta^+=0} + \int d\theta^+ \, (\Phi_+ - \Phi_-) \, \Phi_0 \Psi_0 \big|_{\bar\theta^+=0} + c.c. \tag{5.13}$$

In phase B, when a complex scalar in Φ_0 gets a vev, this superpotential acts as a mass term for P_- and Ψ_+, effectively setting these fields to zero. The variation with respect to Ψ_0 implies

$$(\Phi_+ - \Phi_-) \, \Phi_0 = 0 \tag{5.14}$$

so that either $\Phi_+ - \Phi_- \neq 0$ with $\Phi_0 = 0$ (phase A) or vice versa (phase B).

We believe the two-dimensional phase transition described here is in the same universality class as the phase transition in a simple type IIB brane model that we describe next. It would be nice to understand the relation between these brane models better, e.g. find a precise duality that relates the two.

Hanany-Witten type brane models

Here we propose another brane system that realizes the field theory setup of the 3d $\mathcal{N} = 2$ gauge theory (3.11) with a half-BPS interface (5.12), thus making a full circle back to type IIB string theory and closer to the brane brick models [3–5] that were our original inspiration.

Following [28], we can consider a stack of N D3-branes suspended between two fivebranes in type IIB string theory. We choose one of the fivebranes to be a NS5-brane, with world-volume along directions 012345, and the second fivebrane to be of type (p, q) and oriented along directions $01234[59]_\theta$, where $[59]_\theta$ indicates a rotation in (x^5, x^9) plane by angle θ. It is well known [29–31] that such brane configuration carries 3d $\mathcal{N} = 2$ gauge theory (3.11) on the D3-brane world-volume, provided that

$$n = \frac{p}{q} = \tan\theta \tag{5.15}$$

is an integer (equal to the value of the Chern-Simons coefficient). We assume the world-volume of D3-branes to be along the directions (x^0, x^1, x^2) and x^6:

$$\begin{aligned}
\text{NS5}: &\quad 012345 \\
(p,q)5: &\quad 01234[59]_\theta \\
\text{D3}_+: &\quad 012_+ \quad 6 \\
\text{D3}_-: &\quad 012_- \quad 6 \\
\text{D5}: &\quad 01 \quad 3456
\end{aligned}$$

where in the last line we also included a D5-brane localized along the x^2 direction. This D5-brane breaks half of the supersymmetries of the 3d $\mathcal{N} = 2$ theory on D3-brane, and therefore creates a codimension-1 half-BPS defect.[15] Also indicated in this table, and

JHEP11(2020)033

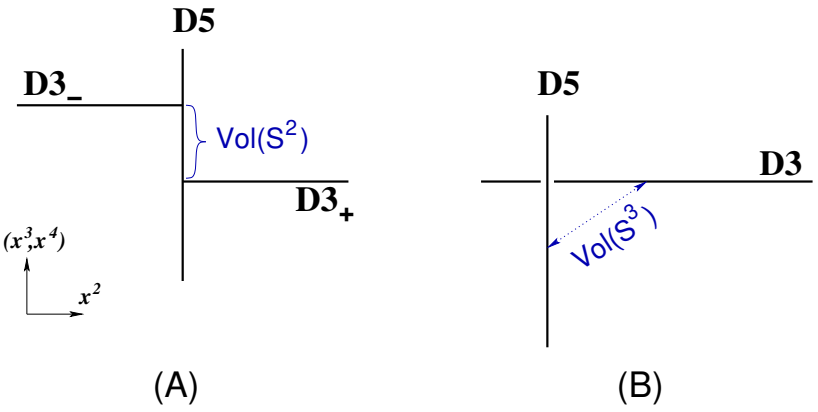

Figure 19. Two phases of a 2d $\mathcal{N} = (0, 2)$ interface (5.7) in a 3d $\mathcal{N} = 2$ theory (3.11).

illustrated in figure 19, is the possibility of D3-brane(s) splitting into two pieces along the D5-brane.

Since the only directions shared by all three fivebranes in our IIB system are (x^0, x^1) and (x^3, x^4), the D3-branes can only separate along (x^3, x^4),

$$\begin{aligned} &\text{Phase A:} \quad \Delta x^3 + i\Delta x^4 = \epsilon = \Phi_+ - \Phi_- \\ &\text{Phase B:} \quad \Delta x^7 + i\Delta x^8 = \Phi_0 \end{aligned} \tag{5.16}$$

Here we identified this separation with the parameters in (5.9) since the physics on the branch parametrized by $\epsilon \neq 0$ matches that of phase A in the above discussion. Similarly, phase B of the 2d $\mathcal{N} = (0, 2)$ theory at the D3-D5 intersection corresponds to moving the D5-brane along the (x^7, x^8) directions, as illustrated on the second panel of figure 19.

It should not be too difficult to generalize this analysis of brane configurations — in M-theory as well as in type IIB string theory — to arbitrary values of n and N. More generally, it is natural to ask: What kinds of topology changing transitions can coassociative 4-manifolds have? We leave these interesting problems to future work.

Acknowledgments

It is pleasure to thank Robert Bryant, Lorenzo Foscolo, Sheldon Katz, Rafe Mazzeo, Jeffrey Meier, Grigory Mikhalkin, and Nathan Seiberg for useful discussions. The work of S.F. is supported by the National Science Foundation grant PHY-1820721. The work of S.G. is supported by the U.S. Department of Energy, Office of Science, Office of High Energy Physics, under Award No. DE-SC0011632, and by the National Science Foundation under Grant No. NSF DMS 1664240. The work of S.L. is supported by Samsung Science and Technology Foundation under Project Number SSTF-BA1402-08.

[15] A similar realization of half-BPS defects in 3d $\mathcal{N} = 2$ super-Chern-Simons theory on D3-branes was considered in [32], though details of the corresponding brane models appear to be different.

JHEP11(2020)033

A Supersymmetry conditions for D6-branes

Here we show that brane configuration (1.7) in type IIA string theory allows adding D6-branes supported on special Lagrangian submanifolds in X, without breaking supersymmetry further. Moreover, and especially important for our applications, the orientation of extra D6-branes needs to be strictly correlated with the orientation of D4-branes; namely, if D4-branes are calibrated by $\mathrm{Re}(e^{i\theta}\Omega)$, then D6-branes must be calibrated by $\mathrm{Im}(e^{i\theta}\Omega)$.

For purposes of analyzing supersymmetry conditions, we can replace X by $\mathbb{C}^3$, with its flat Calabi-Yau structure (2.4), and imitate S by a triple of complex hyperplanes supported at $z_1 = 0$, $z_2 = 0$, and $z_3 = 0$, cf. (1.3). In these conventions, D4-branes are calibrated by the 3-form $\mathrm{Re}(\Omega)$, and the brane configuration looks as follows:

	0	1	2	3	4	5	6	7	8	9
NS5	×	×	×	×	×	×				
NS5′	×	×	×	×			×	×		
NS5″	×	×			×	×	×	×		
D4	×	×	×		×		×			

(A.1)

The supersymmetry condition for a NS5-brane with world-volume along the directions 012345 is given by $\epsilon_{L,R} = -\Gamma^{012345}\epsilon_{L,R}$, and similarly for the other two branes NS5′ and $NS5''$. Here, ϵ_L and ϵ_R are 10d spinors of left and right chirality:

$$\epsilon_L = -\Gamma^{0123456789}\epsilon_L\,, \quad \epsilon_R = +\Gamma^{0123456789}\epsilon_R\,. \tag{A.2}$$

Combining the supersymmetry condition for a D4-brane, $\epsilon_L = \Gamma^{01246}\epsilon_R$, with the above mentioned condition for a NS5-brane, after simple gamma-matrix algebra we obtain $\epsilon_L = \Gamma^{0124789}\epsilon_R$. This is precisely the supersymmetry condition for a D6-brane with world-volume along the directions 0124789. Similarly, combining the D4-brane supersymmetry condition with those for NS5′ and NS5″ branes, we learn that any of the following D6-branes can be introduced into the brane configuration (A.1) without breaking supersymmetry further [33]:

	0	1	2	3	4	5	6	7	8	9
D6	×	×	×		×			×	×	×
D6′	×	×	×			×	×		×	×
D6″	×	×		×	×		×		×	×

(A.3)

Note, all of these D6-branes meet the original D4-branes along two directions inside X, precisely as special Lagrangian submanifolds calibrated by the 3-form $\mathrm{Im}(\Omega)$ (with our convention that D4-branes are calibrated by $\mathrm{Im}(\Omega)$). The other set of D6-branes, with world-volume along directions 0135789 is also calibrated by $\mathrm{Im}(\Omega)$ and, as can be seen directly via gamma-matrix algebra, does not break supersymmetry further.

B Calibration condition

Here we show how to derive the ODE (4.13) from the calibration condition $\Phi|_{M_4} = 0$, $\Psi|_{M_4} = d(\mathrm{vol})_{M_4}$ and the SO(3)-invariant ansatz introduced in section 4. For concreteness, we focus on the case $n = 2$, but generalization to other n is straightforward.

JHEP11(2020)033

Taub-NUT. Introducing n D6-branes replaces $\mathbb{C}^3 \times S^1$ by $\mathbb{R}^3 \times \mathrm{TN}_n$, where TN_n is an n-centered Taub-NUT. Recall that the Taub-NUT metric takes the form

$$ds^2\left(\mathrm{TN}_n\right) = H d\vec{x}^2 + H^{-1}\left(d\widetilde{\psi} + \chi\right)^2 , \quad d\chi = *_3 dH , \tag{B.1}$$

where $*_3$ is the Hodge dual with respect to the flat metric of $\mathbb{R}^3(\vec{x}) = \mathrm{TN}_n/S^1$. The angle variable $\widetilde{\psi}$ has period 4π. We choose the harmonic function H to preserve the SO(3) symmetry in $\mathbb{R}^3(\vec{x})$

$$H = B + \frac{n}{r} , \quad \chi = n\cos\theta d\phi . \tag{B.2}$$

The overall orientation of $\mathbb{R}^3 \times \mathrm{TN}_n$ is fixed by

$$d(\mathrm{vol})_{\mathbb{R}^3\times\mathrm{TN}_n} = dy^{123} \wedge H dx^{123} \wedge \left(d\widetilde{\psi} + \chi\right) = d(\mathrm{vol})_{\mathbb{R}^3} \wedge d(\mathrm{vol})_{\mathrm{TN}_n} . \tag{B.3}$$

When $r \gg 1$, the TN metric asymptotes to $\mathbb{R}^3 \times S^1$ with the circumference of S^1 approaching 4π. When $r \ll 1$, the constant term in H is suppressed and the metric approaches that of $\mathbb{C}^2/\mathbb{Z}_n$,

$$ds^2 \approx d\rho^2 + \frac{\rho^2}{4}\left[d\theta^2 + \sin^2\theta d\phi^2 + (d\psi + \cos\theta d\phi)^2\right] , \quad \psi := \frac{1}{n}\widetilde{\psi} , \quad \rho^2 := (4n)r . \tag{B.4}$$

Associative and co-associative. To obtain the associative 3-form Φ for $\mathbb{R}^3(\vec{y}) \times \mathrm{TN}_n(\vec{x}, \widetilde{\psi})$, we begin with (4.1) and make the replacement,

$$dx^i \to H^{\frac{1}{2}} dx^i , \quad d\psi \to H^{-\frac{1}{2}}\left(d\widetilde{\psi} + \chi\right) , \tag{B.5}$$

so that

$$\begin{aligned} \Psi &= H\left(\frac{1}{2}J \wedge J\right) + \left(H dx^{123} - dy^{ij} \wedge dx^k\right) \wedge (d\widetilde{\psi} + \chi) = d(\mathrm{vol})_{\mathrm{TN}_n} - dy^{ij} \wedge \omega^k , \\ \Phi &= J \wedge (d\widetilde{\psi} + \chi) + dy^{123} - H\left(dy^k \wedge dx^{ij}\right) = d(\mathrm{vol})_{\mathbb{R}^3_y} - dy^k \wedge \omega^k . \end{aligned} \tag{B.6}$$

We introduced the well-known self-dual 2-forms on TN_n,

$$\omega^k = H dx^{ij} + dx^k \wedge \left(d\widetilde{\psi} + \chi\right) , \qquad d\omega^k = 0 , \quad *_{\mathrm{TN}}\left(\omega^k\right) = +\omega^k , \tag{B.7}$$

and a few short-hand notations:

$$\begin{aligned} dx^{123} &= dx^1 \wedge dx^2 \wedge dx^3 , \\ dx^k \wedge dy^{ij} &= dx^1 \wedge \left(dy^2 \wedge dy^3\right) + dx^2 \wedge \left(dy^3 \wedge dy^1\right) + dx^3 \wedge \left(dy^1 \wedge dy^2\right) , \\ dy^k \wedge \omega^k &= dy^1 \wedge \omega^1 + dy^2 \wedge \omega^2 + dy^3 \wedge \omega^3 . \end{aligned} \tag{B.8}$$

Other notations are understood in similar ways. Clearly, $d\omega^k = 0$ implies $d\Psi = 0 = d\Phi$.

JHEP11(2020)033

Embedding ansatz. We embed M_4 into $\mathbb{R}^3 \times \mathrm{TN}_2$ by expressing $\vec{y}$ as functions of $(\vec{x}, \widetilde{\psi})$. It is more convenient to use polar coordinates (r, θ, ϕ, ψ), where $r = |\vec{x}|$ and (θ, ϕ, ψ) are the standard angle coordinates on S^3. The ψ here is related to $\widetilde{\psi}$ in (B.1) by

$$\widetilde{\psi} = n\psi = 2\psi \,. \tag{B.9}$$

We choose specific coordinates in the unit quaternion/spinor description of S^3,

$$q = \begin{pmatrix} u_1 & -\overline{u}_2 \\ u_2 & \overline{u}_1 \end{pmatrix} , \quad u = \begin{pmatrix} u_1 \\ u_2 \end{pmatrix} = \begin{pmatrix} \cos(\theta/2) e^{i(-\psi-\phi)/2} \\ \sin(\theta/2) e^{i(-\psi+\phi)/2} \end{pmatrix} , \quad \widetilde{u} = \begin{pmatrix} -\overline{u}_2 \\ \overline{u}_1 \end{pmatrix} . \tag{B.10}$$

The associated invariant 1-forms are

$$\begin{aligned} \vec{\tau} &= i \,\mathrm{Tr}\left(\vec{\sigma} q^\dagger dq\right) \\ &= (\sin\psi d\theta - \cos\psi \sin\theta d\phi, \cos\psi d\theta + \sin\psi \sin\theta d\phi, d\psi + \cos\theta d\phi) \,. \end{aligned} \tag{B.11}$$

They satisfy

$$d\tau_i = -\frac{1}{2}\epsilon^{ijk}(\tau_j \wedge \tau_k) \,, \quad \tau_1 \wedge \tau_2 \wedge \tau_3 = \sin\theta (d\theta \wedge d\phi \wedge d\psi) \,. \tag{B.12}$$

The $\vec{x}$ coordinates are mapped to (r, θ, ϕ) coordinates in the usual way,

$$\vec{x} = r\,\widehat{m} \,, \quad \widehat{m} = u^\dagger \vec{\sigma} u = (\sin\theta\cos\phi, \sin\theta\sin\phi, \cos\theta) \,, \tag{B.13}$$

such that

$$d\vec{x}^2 = dr^2 + r^2 d\widehat{m}^2 = dr^2 + r^2(\tau_1^2 + \tau_2^2) = dr^2 + r^2(d\theta^2 + \sin^2\theta d\phi^2) \,. \tag{B.14}$$

As stated in (4.11), we look for an ansatz of the form

$$\vec{y} = g(r)\widehat{n}(\theta, \phi, \psi) \,, \quad \widehat{n} \cdot \widehat{n} = 1 \,, \quad \widehat{m} \cdot \widehat{n} = 0 \,. \tag{B.15}$$

Such a fibration is readily achieved by means of the spinor

$$v = \frac{1}{\sqrt{2}}(u + \widetilde{u}) \,, \tag{B.16}$$

such that

$$\widehat{n} = v^\dagger \vec{\sigma} v = \cos\psi(\cos\theta\cos\phi, \cos\theta\sin\phi, -\sin\theta) + \sin\psi(-\sin\phi, \cos\phi, 0) \,. \tag{B.17}$$

We note that, somewhat similarly to (B.14),

$$d\widehat{n}^2 = \tau_2^2 + \tau_3^2 \,. \tag{B.18}$$

JHEP11(2020)033

Calibration condition. We want M_4 to be a coassociative 4-cycle, that is,

$$\Phi|_{M_4} = 0\,, \quad \Psi|_{M_4} = d(\mathrm{vol})_{M_4}\,. \tag{B.19}$$

Our goal is to obtain a first-order non-linear ODE for $g(r)$ from the first condition.

The angular part is fixed by the $\mathrm{SO}(3) \times \mathrm{U}(1)$ symmetry. To see it clearly, it is useful to rewrite dm^k and dn^kas linear combinations of τ_i. In a local orthonormal frame spanned by $\widehat{m}$, $\widehat{n}$ and $\widehat{\ell} := \widehat{m} \times \widehat{n}$, we have

$$dm^k = n^k\tau_2 - \ell^k\tau_1\,, \quad dn^k = \ell^k\tau_3 - m^k\tau_2\,, \quad d\ell^k = m^k\tau_1 - n^k\tau_3\,. \tag{B.20}$$

It follows that

$$\begin{aligned} m^i dm^j - m^j dm^i &= n^k\tau_1 + \ell^k\tau_2\,, & dm^i \wedge dm^j &= m^k(\tau_1 \wedge \tau_2)\,, \\ n^i dn^j - n^j dn^i &= \ell^k\tau_2 + m^k\tau_3\,, & dn^i \wedge dn^j &= n^k(\tau_2 \wedge \tau_3)\,. \end{aligned} \tag{B.21}$$

Let us compute the pull-back of Φ onto M_4:

$$\Phi = dy^{123} - dy^k \wedge \omega^k = dy^{123} - dy^k \wedge \Big(H dx^{ij} + 2\, dx^k \wedge \tau_3\Big)\,. \tag{B.22}$$

With the coordinates (B.13) and the ansatz (B.15), we have

$$\begin{aligned} dx^k &= m^k dr + r\,\Big(dm^k\Big) = m^k dr + r\,\Big(n^k\tau_2 - \ell^k\tau_1\Big)\,, \\ dy^k &= g' n^k dr + g\,\Big(dn^k\Big) = g' n^k dr + g\,\Big(\ell^k\tau_3 - m^k\tau_2\Big)\,, \end{aligned} \tag{B.23}$$

so that

$$dx^{123} = r^2 dr(\tau_1 \wedge \tau_2)\,, \quad dy^{123} = g^2 g' dr(\tau_2 \wedge \tau_3)\,. \tag{B.24}$$

The two-forms ω_k get pulled back to

$$\begin{aligned} \omega_k &= Hr dr \wedge (m^i dm^j - m^j dm^i) + Hr^2(dm^i \wedge dm^j) \\ &\quad + 2m^k dr \wedge \tau_3 + 2r\, dm^k \wedge \tau_3 \\ &= dr \wedge \Big[(Hr)(n^k\tau_1 + \ell^k\tau_2) + 2m^k\tau_3\Big] \\ &\quad + \Big[(Hr^2)m^k(\tau_1 \wedge \tau_2) + (2r)\{\ell^k(\tau_3 \wedge \tau_1) + n^k(\tau_2 \wedge \tau_3)\}\Big]\,. \end{aligned} \tag{B.25}$$

In Φ, one may naively expect a $(\tau_1 \wedge \tau_2 \wedge \tau_3)$ term and three $dr \wedge (\tau_i \wedge \tau_j)$ terms. It turns out that all but the $dr \wedge (\tau_2 \wedge \tau_3)$ terms vanish. Collecting all contributions, and demanding $\Phi|_{M_4} = 0$, we finally obtain the desired ODE for $n = 2$:

$$g^2 g' - (Hr)g - 2rg' - 2g = 0 \quad \Longleftrightarrow \quad g' = \frac{(Hr+2)g}{g^2 - 2r}\,. \tag{B.26}$$

JHEP11(2020)033

References

[1] P.S. Aspinwall et al., *Dirichlet branes and mirror symmetry*, vol. 4 of *Clay Mathematics Monographs*, American Mathematical Society, Providence, RI, Clay Mathematics Institute, Cambridge, MA, U.S.A. (2009).

[2] A. Butscher, *Deformations of minimal Lagrangian submanifolds with boundary*, *Proc. Am. Math. Soc.* **131** (2003) 1953.

[3] S. Franco, S. Lee and R.-K. Seong, *Brane Brick Models, Toric Calabi-Yau 4-Folds and 2d (0,2) Quivers*, *JHEP* **02** (2016) 047 [arXiv:1510.01744] [INSPIRE].

[4] S. Franco, S. Lee and R.-K. Seong, *Brane brick models and 2d (0, 2) triality*, *JHEP* **05** (2016) 020 [arXiv:1602.01834] [INSPIRE].

[5] S. Franco, S. Lee, R.-K. Seong and C. Vafa, *Brane Brick Models in the Mirror*, *JHEP* **02** (2017) 106 [arXiv:1609.01723] [INSPIRE].

[6] E. Witten, *Solutions of four-dimensional field theories via M-theory*, *Nucl. Phys. B* **500** (1997) 3 [hep-th/9703166] [INSPIRE].

[7] M. Atiyah, J.M. Maldacena and C. Vafa, *An M-theory flop as a large N duality*, *J. Math. Phys.* **42** (2001) 3209 [hep-th/0011256] [INSPIRE].

[8] M. Atiyah and E. Witten, *M theory dynamics on a manifold of G_2 holonomy*, *Adv. Theor. Math. Phys.* **6** (2003) 1 [hep-th/0107177] [INSPIRE].

[9] S. Gukov and J. Sparks, *M theory on spin(7) manifolds. 1*, *Nucl. Phys. B* **625** (2002) 3 [hep-th/0109025] [INSPIRE].

[10] S. Gukov, J. Sparks and D. Tong, *Conifold transitions and five-brane condensation in M-theory on spin(7) manifolds*, *Class. Quant. Grav.* **20** (2003) 665 [hep-th/0207244] [INSPIRE].

[11] M. Bershadsky, C. Vafa and V. Sadov, *D-branes and topological field theories*, *Nucl. Phys. B* **463** (1996) 420 [hep-th/9511222] [INSPIRE].

[12] K. Becker, M. Becker, D.R. Morrison, H. Ooguri, Y. Oz and Z. Yin, *Supersymmetric cycles in exceptional holonomy manifolds and Calabi-Yau 4 folds*, *Nucl. Phys. B* **480** (1996) 225 [hep-th/9608116] [INSPIRE].

[13] M. Blau and G. Thompson, *Aspects of $N_T \geq 2$ topological gauge theories and D-branes*, *Nucl. Phys. B* **492** (1997) 545 [hep-th/9612143] [INSPIRE].

[14] R. Fintushel and R.J. Stern, *Knots, links, and 4-manifolds*, *Invent. Math.* **134** (1998) 363.

[15] A. Gadde, S. Gukov and P. Putrov, *Fivebranes and 4-manifolds*, *Prog. Math.* **319** (2016) 155 [arXiv:1306.4320] [INSPIRE].

[16] L. Foscolo, M. Haskins and J. Nordström, *Complete non-compact G2-manifolds from asymptotically conical Calabi-Yau 3-folds*, arXiv:1709.04904 [INSPIRE].

[17] L. Foscolo, M. Haskins and J. Nordström, *Infinitely many new families of complete cohomogeneity one G2-manifolds: G2 analogues of the Taub-NUT and Eguchi-Hanson spaces*, arXiv:1805.02612 [INSPIRE].

[18] R. Harvey and H.B. Lawson Jr., *Calibrated geometries*, *Acta Math.* **148** (1982) 47 [INSPIRE].

[19] I.A. Bandos, A. Nurmagambetov and D.P. Sorokin, *The Type IIA NS5-brane*, *Nucl. Phys. B* **586** (2000) 315 [hep-th/0003169] [INSPIRE].

JHEP11(2020)033

[20] B.S. Acharya and C. Vafa, *On domain walls of $N = 1$ supersymmetric Yang-Mills in four-dimensions*, hep-th/0103011 [INSPIRE].

[21] S. Gukov, C. Vafa and E. Witten, *CFT's from Calabi-Yau four folds*, *Nucl. Phys. B* **584** (2000) 69 [*Erratum ibid.* **608** (2001) 477] [hep-th/9906070] [INSPIRE].

[22] L. Foscolo, *Complete non-compact* Spin(7) *manifolds from self-dual Einstein 4-orbifolds*, arXiv:1901.04074 [INSPIRE].

[23] D.S. Freed and E. Witten, *Anomalies in string theory with D-branes*, *Asian J. Math.* **3** (1999) 819 [hep-th/9907189] [INSPIRE].

[24] M. Dedushenko, S. Gukov and P. Putrov, *Vertex algebras and 4-manifold invariants*, arXiv:1705.01645 [INSPIRE].

[25] E. Witten, *Duality relations among topological effects in string theory*, *JHEP* **05** (2000) 031 [hep-th/9912086] [INSPIRE].

[26] R. Dijkgraaf, L. Hollands, P. Sulkowski and C. Vafa, *Supersymmetric gauge theories, intersecting branes and free fermions*, *JHEP* **02** (2008) 106 [arXiv:0709.4446] [INSPIRE].

[27] B. Feigin and S. Gukov, *VOA[M_4]*, *J. Math. Phys.* **61** (2020) 012302 [arXiv:1806.02470] [INSPIRE].

[28] A. Hanany and E. Witten, *Type IIB superstrings, BPS monopoles, and three-dimensional gauge dynamics*, *Nucl. Phys. B* **492** (1997) 152 [hep-th/9611230] [INSPIRE].

[29] N. Ohta and P.K. Townsend, *Supersymmetry of M-branes at angles*, *Phys. Lett. B* **418** (1998) 77 [hep-th/9710129] [INSPIRE].

[30] T. Kitao, K. Ohta and N. Ohta, *Three-dimensional gauge dynamics from brane configurations with (p,q)-fivebrane*, *Nucl. Phys. B* **539** (1999) 79 [hep-th/9808111] [INSPIRE].

[31] O. Bergman, A. Hanany, A. Karch and B. Kol, *Branes and supersymmetry breaking in three-dimensional gauge theories*, *JHEP* **10** (1999) 036 [hep-th/9908075] [INSPIRE].

[32] A. Armoni and V. Niarchos, *Defects in Chern-Simons theory, gauged WZW models on the brane, and level-rank duality*, *JHEP* **07** (2015) 062 [arXiv:1505.02916] [INSPIRE].

[33] H. Garcia-Compean and A.M. Uranga, *Brane box realization of chiral gauge theories in two-dimensions*, *Nucl. Phys. B* **539** (1999) 329 [hep-th/9806177] [INSPIRE].

JHEP11(2020)033